

Robust Device-Independent Quantum Key Distribution

René Schwonnek,^{1,*} Koon Tong Goh,^{1,*} Ignatius W. Primaatmaja,² Ernest Y.-Z. Tan,³ Ramona Wolf,⁴ Valerio Scarani,^{2,5} and Charles C.-W. Lim^{1,2,†}

¹*Department of Electrical & Computer Engineering, National University of Singapore, Singapore*

²*Centre for Quantum Technologies, National University of Singapore, Singapore*

³*Institute for Theoretical Physics, ETH Zürich, Switzerland*

⁴*Institut für Theoretische Physik, Leibniz Universität Hannover, Germany*

⁵*Department of Physics, National University of Singapore, Singapore*

Device-independent quantum key distribution (DIQKD) is the art of using untrusted devices to distribute secret keys in an insecure network. It thus represents the ultimate form of cryptography, offering not only information-theoretic security against channel attacks, but also against attacks exploiting implementation loopholes. In recent years, much progress has been made towards realising the first DIQKD experiments, but current proposals are just out of reach of today's loophole-free Bell experiments. In this Letter, we close the gap between the theory and practice of DIQKD with a simple variant of the original protocol based on the celebrated Clauser-Horne-Shimony-Holt (CHSH) Bell inequality. In using two randomly chosen key generating bases instead of one, we show that the noise tolerance of DIQKD can be significantly improved. In particular, the extended feasibility region now covers some of the most recent loophole-free CHSH experiments, hence indicating that the first realisation of DIQKD already lies within the range of these experiments.

The basic task of DIQKD [1, 2] is to distribute a pair of identical secret keys between two users, called Alice and Bob, who are embedded in an untrusted network. To help them in their task, Alice and Bob are each given a measurement device, which they use to perform random measurements on a sequence of entangled systems provided by an adversary called Eve (see Fig. 1). The main advantage of DIQKD is that the measurement devices need not be characterised—Alice and Bob only need to verify that the input-output statistics of the devices violate a CHSH Bell inequality [3, 4]. As such, DIQKD represents the pinnacle of cryptography in terms of the number of assumptions required. More specifically, it only asks that (1) the users each hold a trusted source of local randomness, (2) their laboratories are well isolated, (3) they use trusted algorithms for processing their measurement data, and that (4) quantum theory is correct. Given these basic assumptions (which are in fact standard assumptions in cryptography), one can then show that DIQKD is information-theoretically secure [1, 5, 6].

The practical implementation of DIQKD, however, remains a major scientific challenge. This is mainly due to the need to have extremely good channel parameters (i.e., high Bell violation and low bit error rate), which in practice requires ultra-low-noise setups with very high detection efficiencies; though in recent years the gap between the theory and practice has been significantly reduced owing to more powerful proof techniques [5–7] and the demonstrations of loophole-free Bell experiments [8–11]. The present gap is best illustrated by Murta et al. [12], whose feasibility study showed that current loophole-free Bell experiments are just short of generating positive key rates assuming the original DIQKD protocol [1, 2] (see the dashed line in Fig. 3). To

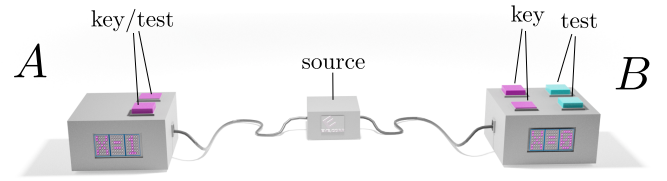


Fig. 1. **Robust DIQKD:** Alice and Bob use uncharacterised devices to perform measurements on a quantum state that is created by a source that is potentially controlled by an adversary (Eve). In the proposed protocol, Alice has two possible inputs (measurement settings, magenta buttons) which are used for key generation and for running the CHSH Bell test, and Bob has four possible inputs grouped into two sets (magenta/cyan buttons): the magenta buttons are used for key generation while the cyan buttons are used for running the CHSH Bell test.

improve the robustness of DIQKD, researchers have taken several approaches, from heralded qubit amplifiers [13, 14], local Bell tests [15], to two-way classical protocols [16]. However, none of these proposals are truly practical, for they are either more complex in implementation or provide only very little improvements in the channel parameters.

Here, we show that a simple variant of the original DIQKD protocol is enough to obtain significant improvements in the channel parameters. To start with, we note that in the original protocol introduced by Acín et al. [2], the key generating basis is predetermined and known to Eve. For concreteness, let Alice's and Bob's measurement settings be denoted by $X \in \{0, 1\}$ and $Y \in \{0, 1, 2\}$, respectively, and let the corresponding outcomes be denoted by $A_X \in \{0, 1\}$ and $B_Y \in \{0, 1\}$. The secret key is derived from the events in which Alice and Bob choose $X = 0$ and $Y = 0$, respectively. The remaining measurement combinations are then used for determining the CHSH violation. Our DIQKD proposal is essentially the same as the original protocol, except that we introduce an additional

* These authors contributed equally to this work.

† charles.lim@nus.edu.sg

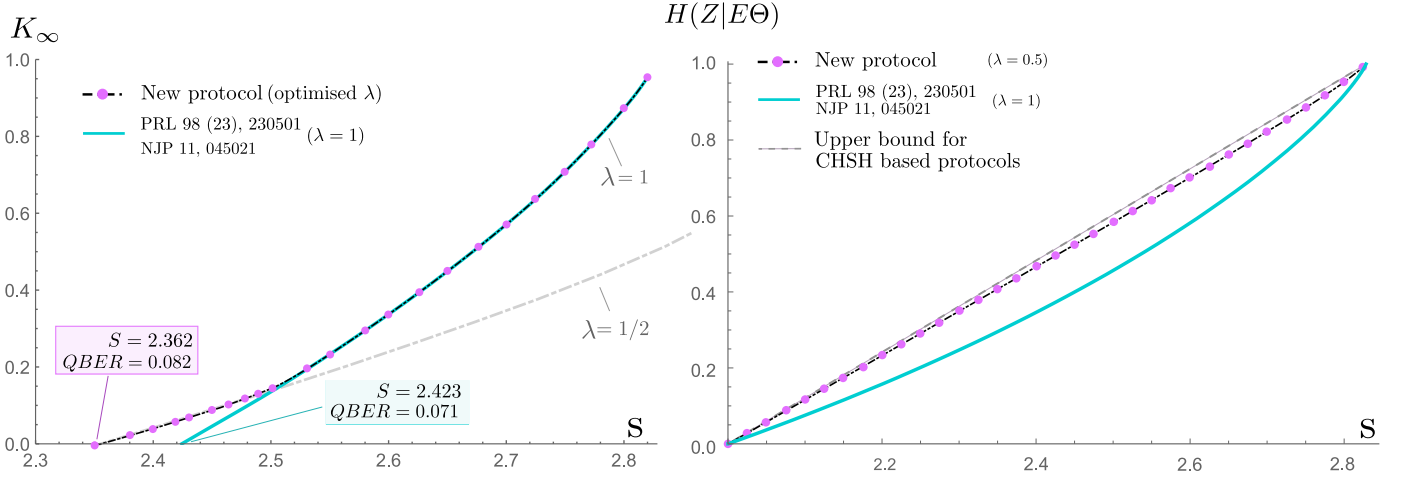


Fig. 2. **Secret key rate and uncertainty of Eve:** (right) Assuming quantum theory, collective attacks, and a given CHSH value $S > 2$, we show that our new protocol can establish and certify drastically more uncertainty $H(Z|E\Theta)$ (close to the upper physical limit) than the best approach known before. (left) We consider a noise model (depolarising noise) [1, 2] that only depends on the CHSH value S . Now a larger amount of noise can be tolerated in order to establish a positive key rate K_∞ . In detail we can decrease the critical CHSH value from 2.423 to 2.362. This corresponds to an increase of the critical bit-error-rate from 0.071 to 0.082, which brings a practical implementation of DIQKD into the reach of existing experiments.

measurement setting for Bob and now generate the secret key from both of Alice's measurements. This additional setting is needed so that Bob has a measurement that is aligned with Alice's additional key generating basis to obtain correlated outcomes (like in the case of the original protocol). Hence in our proposal, the key generation events are those whereby Alice and Bob choose $X = Y = 0$ and $X = Y = 1$. Below, we describe the proposal in detail.

1. Measurements. This step is carried out in N rounds, where N is assumed to be asymptotically large. In each measurement round, Alice's and Bob's inputs, denoted by $X \in \{0, 1\}$ and $Y \in \{0, 1, 2, 3\}$, respectively, are drawn according to the following probability distributions: $P(X = 0) = p$, $P(X = 1) = 1 - p$, $P(Y = 0) = qp$, $P(Y = 1) = q(1 - p)$ and $P(Y = 2) = P(Y = 3) = (1 - q)/2$, where $0 \leq p, q \leq 1$. Once Alice and Bob enter their inputs into their respective devices, they each obtain a measurement outcome, which we denote by $A_X \in \{0, 1\}$ and $B_Y \in \{0, 1\}$ respectively.

2. Sifting. Alice and Bob announce their measurement inputs over an authenticated public channel. This allows them to identify two common subsets of their measurement data: a pair of *raw keys* [17] of size $\sim q(p^2 + (1 - p)^2)N$ (corresponding to $Y \in \{0, 1\}$ and $X = Y$) and a pair of parameter estimation data of size $\sim (1 - q)N$ (corresponding to $Y \in \{2, 3\}$). Alice and Bob discard the remaining measurement data.

3. Parameter estimation. Alice and Bob publicly reveal their measurement outcomes from the parameter estimation data set and compute the underlying CHSH value:

$$S = \max\{2, C_{12} - C_{02} - C_{03} - C_{13}\}, \quad (1)$$

where $C_{XY} = P(A_X = B_Y|X, Y) - P(A_X \neq B_Y|X, Y)$ is the correlation function of X, Y . Alice and Bob proceed to the next step if $S > S_{\text{tol}}$, where S_{tol} is a predefined threshold value. Otherwise, they abort the protocol.

4. One-way error correction and verification. In the first part, Alice computes a syndrome based on her raw key (denoted by $Z_1 Z_2 \dots$) and sends it to Bob via the public channel, who then uses the syndrome and his raw key to recover Alice's key. In the second part, they perform an error verification by comparing the hash values of their raw keys. Alice and Bob proceed to privacy amplification if the hash values are identical, otherwise they abort the protocol.

5. Privacy amplification. Alice and Bob perform privacy amplification to remove Eve's information about Alice's raw key. Once this is completed, Alice and Bob are left with a pair of identical secret keys.

It is well known that incompatible measurements are necessary for the violation of a Bell inequality and that such measurements are not jointly measurable and hence cannot admit a joint distribution [18–20]. The intuition behind our proposal roughly follows along this line and exploits two related facts: (1) the key generation measurements of Alice must be incompatible for $S > 2$ and (2) Eve has to guess the secret key from two randomly chosen incompatible measurements.

When the secret key is only generated from a single measurement, like in the original DIQKD protocol, Eve's attacks are basically limited only by the observed CHSH violation and thus the monogamy of entanglement [21]. Eve, however, knows which measurement is used for key generation and hence can optimise her attack accordingly. On the other hand, if the secret key is generated from a random

choice of two possible measurements, Eve faces an additional difficulty. Namely, in order to achieve a CHSH violation, the two measurements cannot be the same, and it is known [1] that for CHSH-based protocols, different measurements can give Eve different amounts of side-information; note that this is not the case for BB84 and six-state QKD protocols. Therefore, at least one of the measurements will not be the one that maximises Eve's side-information, giving an advantage over protocols based only on one key-generating measurement (Eve cannot tailor her attack to the measurement in each round individually, since she does not know beforehand which measurement will be chosen).

In the following, we quantify the security of the protocol using the asymptotic secret key rate, K_∞ , assuming collective attacks (the generalisation to general attacks is discussed below). This quantity is the ratio of the extractable secret key length to the total number of measurement rounds, N , where $N \rightarrow \infty$. In the asymptotic limit, we may also take $q \rightarrow 1$, which maximises the so-called *sifting factor* and get

$$K_\infty = p_s r_\infty,$$

where $p_s := p^2 + (1-p)^2$ is the probability of having matching key bases, and r_∞ is the secret fraction [17]. The latter is given in terms of entropic quantities and reads

$$r_\infty := \underbrace{\lambda H(A_0|E) + (1-\lambda)H(A_1|E)}_{H(Z|E\Theta)} - \lambda h(Q_{A_0 B_0}) - (1-\lambda)h(Q_{A_1 B_1}), \quad (2)$$

where $h(x) := -x \log(x) - (1-x) \log(1-x)$ is the binary entropy function, $\lambda := p^2/p_s$, $Q_{A_X B_Y} := P(A_X \neq B_Y | X, Y)$ is the quantum bit error rate (QBER) for X, Y , and E is Eve's quantum side-information gathered just before the error correction step. Here, $Z = A_\Theta$ and $\Theta \in \{0, 1\}$ is the random variable denoting Alice's basis choice conditioned on the event either $X = Y = 0$ or $X = Y = 1$. The second line in equation (2) is the amount of information leaked to Eve during the error correction step (decoding with side-information Θ).

The main challenge here is to put a reliable lower bound on the conditional von Neumann entropy $H(Z|E\Theta)$, which measures the amount of uncertainty Eve has about Z given side-information $E\Theta$, using solely the observed CHSH violation, S . To this end, we employ a family of device-independent entropic uncertainty relations [22, 23], which we can solve efficiently and reliably using a short sequence of numerical computations. More specifically, we seek to establish weighted entropic inequalities of the form

$$\lambda H(A_0|E) + (1-\lambda)H(A_1|E) \geq C^*(S),$$

where $C^*(S)$ is a function of the observed CHSH violation, S . A proof sketch is outlined in the Methods section and the complete analysis is provided in the accompanied supplementary information.

A commonly used noise model for benchmarking the security performance of different QKD protocols is the depolarising channel model [1, 2, 17]. In this noise model, all

QBERs are the same and related to the CHSH value S via

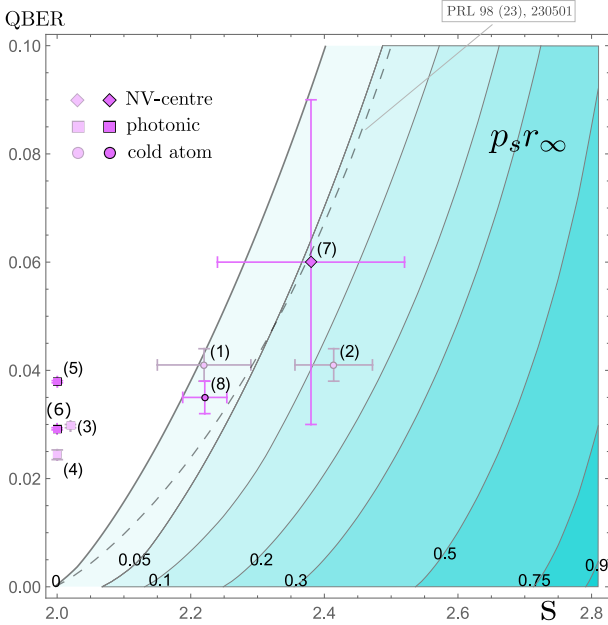
$$Q_{A_0 B_0} = Q_{A_1 B_1} = Q = \frac{1}{2} \left(1 - \frac{S}{2\sqrt{2}} \right).$$

Using this model, we compute the secret key rate and $H(Z|E\Theta)$, which are presented in Fig. 2. Here, λ is a free parameter (i.e., a protocol parameter) that can be optimised by Alice and Bob (i.e., they optimise $p = P(X = 0)$) for a given pair of (S, Q) . The result of this optimisation is remarkably simple: it is optimal to use a protocol with $\lambda = 1/2$ (uniformly random key generation bases) if $S \lesssim 2.5$ (high noise) and set $\lambda = 1$, i.e., a fixed key generation basis otherwise (low noise). Surprisingly, there is no need to consider the intermediate values of $1/2 < \lambda < 1$.

In the case of the latter, our proposal reverts back to that of Acín et al. [1, 2] and the computed secret key rate appears to exactly match their analytical key rate bound. When using $H(Z|E\Theta)$ as a performance metric (which only depends on S and thus applies to a general class of channel models satisfying this constraint), we observe that the uncertainty of Eve for our proposal is always higher than that of the original protocol for all $S \in (2, 2\sqrt{2})$, see the right side of Fig. 2. In fact, our proposal is nearly optimal, in the sense that it is nearly identical to the linear bound, which is the fundamental upper limit of Eve's uncertainty given a fixed S .

In order to evaluate the feasibility of our proposal, we look at the existing list of loophole-free CHSH experiments [12] and compute the corresponding secret key rates. Generally speaking, there are two types of Bell experiments: one based on measuring entangled photon pairs using high efficiency single-photon detectors and the other based on event-ready systems [30] using entanglement swapping between entangled photon pairs and atoms/NV-centres. Following along the lines of Murta et al. [12], we prepare a feasibility region plot for the list of CHSH experiment therein, which is presented in Fig. 3. The immediate observation is that our DIQKD proposal significantly expands the region of channel parameters that give rise to positive key rates, thus substantially improving the robustness of DIQKD. The next observation is that event-ready loophole-free CHSH experiments [8, 11] are now well within the positive key region; as opposed to the original protocol where they are either in the insecure region or around the boundary. Unfortunately, CHSH experiments based on entangled photon pairs are still in the insecure region, although it should be mentioned that this observation holds only for our proposal and the original DIQKD protocol.

While our results clearly indicate that the first realisation of DIQKD is now well within the grasp of recent event-ready CHSH experiments, there are still a few potential issues. For one, we note that these experiments are pretty slow, e.g., the event-ready experiment by Hensen et al. [8] performed only 245 rounds of measurement during a total collection time of 220 h. This has an important implication on the finite-key analysis of DIQKD as it has been estimated that at least 10^6 measurement rounds are needed to achieve positive keys [12]. Recently, Humphreys et al. [31]



demonstrated that it is possible to improve the entanglement rate by couple of orders of magnitude, but this comes at the expense of the overall state fidelity and hence lower CHSH violations. While this is a predicament for the original DIQKD protocol, our proposal with increased robustness could enable some of these faster event-ready experiments to achieve positive keys with lower CHSH violations in the finite-key regime.

The above also brings us to the study of finite-size effects of our DIQKD proposal. In our security analysis, we made the assumption of collective attacks and provided a concise numerical method to reliably lower bound $H(Z|E\Theta)$, the von Neumann entropy of Z given $E\Theta$. We argue that there is likely no loss of generality in taking this approach, as it may be possible to extend the results to general attacks in the finite-key regime using the entropy accumulation theorem [32–34]. This was indeed the case for the original DIQKD protocol, where the collective attack analysis has been extended to general attacks in the finite-key regime [6]. We thus leave the finite-key analysis of our proposal (with a detailed modelling of event-ready Bell experiment) for future work.

To further improve the robustness of DIQKD, there are a few possible directions to take. For one, we can consider the full input-output probability distribution instead of just taking the CHSH violation, which only looks at part of the available information. This suggests that the secret key rates presented in Fig. 3 could be further improved by using the full probability distribution. More secrecy could be certified if one finds a method to compute secret key rates which factors into account the full probability distribution estimated from the experiment. A method for doing so was recently developed [35]; however, we found that the bounds it gives in this scenario (see supplementary information) do not outperform those shown above.

label	experiment	year	rate [bit]
(1)	Matsukevich et al. [24]	2008	0.004
(2)	Pironio et al., [25]	2010	0.118
(3)	Giustina et al. [26]	2013	0
(4)	Christensen et al. [27]	2013	0
(5)	Giustina et al. [9]	2015	0
(6)	Shalm et al. [10]	2015	0
(7)	Hensen et al. [8]	2015	0.057
(8)	Rosenfeld et al. [11]	2017	0.019

Fig. 3. **Achievable rates for existing experiments:** The contour plot to the left illustrates the keyrate $K_\infty = p_s r_\infty$ as a function of S and $QBER$. We marked the location of eight recent experiments (data from Murta et al. [12], Tab. 4). The experiments (1-4) (marked in grey) are not loophole-free. The dashed line marks the boundary of the previously known [1, 2] zero-key-rate region. Our DIQKD proposal suggests that now a positive key rate with relevant magnitude is possible for all non-photonic experiments ((1,2) and (7,8)). However, note that the value of $QBER$ for experiment (8) provided by Murta et al. [12] is based on the experiment of Henkel et al. [28] while the $QBER$ achievable by experiment (8) is estimated to be higher [29].

ACKNOWLEDGMENTS

R. S., K.-T. G., and C. C.-W. L. were funded by the National Research Foundation of Singapore, under its NRF Fellowship grant (NRFF11-2019-0001) and NRF Quantum Engineering Programme grant (QEP-P2), and the Centre for Quantum Technologies. V. S. and I.-W. P. were supported by NRF and the Ministry of Education, Singapore, under the Research Centres of Excellence program. E. Y.-Z. T. was funded by the Swiss National Science Foundation via the National Center for Competence in Research for Quantum Science and Technology (QSIT), the Air Force Office of Scientific Research (AFOSR) via grant FA9550-19-1-0202, and the QuantERA project eDICT. R. W. was supported by the Deutsche Forschungsgemeinschaft (DFG, German Research Foundation) through SFB 1227 (DQ-mat), the RTG 1991, and under Germany’s Excellence Strategy – EXC-2123 QuantumFrontiers – 390837967.

METHODS

Here, we outline the main ideas of our security analysis. The core of the security analysis is a reliable lower-bound estimate on the conditional von Neumann entropy of Eve. The complete analysis is deferred to the accompanying supplementary information.

Average secret key rate

Conditioned on the key generation rounds, Alice and Bob would pick their inputs (basis choices) according to a probability distribution $(p, 1 - p)$. As discussed in the main text, this distribution acts as a free parameter in our protocol and has to be adapted to a given set of channel param-

ters (S, Q) in order to obtain an optimal performance. In the following we will therefore outline how the final key rate K_∞ and secret fraction r_∞ are given as functions of (p, S, Q) .

The secret fraction in a round of the protocol, in which the measurements A_X and B_Y are obtained, can be computed using the Devetak-Winter bound [36] under the assumption of collective attacks,

$$r_\infty^{A_X B_Y} \geq H(A_X|E) - H(A_X|B_Y). \quad (3)$$

Here the term $H(A_X|B_Y)$ only depends on the statistics of the measured data of Alice and Bob, and can therefore be directly estimated in an experiment. For binary measurements this quantity can be furthermore expressed by the respective bit error rate $Q_{A_X B_Y}$ via

$$H(A_X|B_Y) \leq h(Q_{A_X B_Y}). \quad (4)$$

In our protocol, a key generation round is obtained whenever Alice and Bob perform measurements A_X and B_Y with $X = Y$. The probability that Alice and Bob perform the measurements A_0 and B_0 is p^2 and the probability that they perform A_1 and B_1 is $(1-p)^2$. When the error correction is done for both cases, (A_0, B_0) or (A_1, B_1) , separately, we obtain the overall asymptotic key rate as sum of the individual secret fractions weighted by their respective probability. This gives

$$\begin{aligned} K_\infty &\geq p^2 r_\infty^{A_0 B_0} + (1-p)^2 r_\infty^{A_1 B_1} \\ &= p^2 H(A_0|E) + (1-p)^2 H(A_1|E) \\ &\quad - p^2 H(A_0|B_0) - (1-p)^2 H(A_1|B_1) \\ &\geq p_s (\lambda H(A_0|E) + (1-\lambda) H(A_1|E) \\ &\quad - \lambda h(Q_{A_0 B_0}) - (1-\lambda) h(Q_{A_1 B_1})) \\ &:= p_s r_\infty, \end{aligned} \quad (5)$$

where the success probability p_s and the relative distribution of the basis choices $(\lambda, (1-\lambda))$ are given by

$$p_s = (p^2 + (1-p)^2) = 1 - 2p + 2p^2 \quad (6)$$

and

$$\lambda = \frac{p^2}{1 - 2p + 2p^2}, \quad (7)$$

respectively. As mentioned in the main text we also write

$$H(Z|E\Theta) := \lambda H(A_0|E) + (1-\lambda) H(A_1|E) \quad (8)$$

where Θ denotes a binary random variable (distributed by $(\lambda, (1-\lambda))$) that (virtually) determines which basis pair, (A_0, B_0) or (A_1, B_1) , is picked in a successful key generation round in order to generate the values of a combined random variable $Z = A_\Theta$.

Device independent entropic uncertainty relation

The only term in the key rate formula (5) that cannot be directly obtained from the measurement data is the conditional entropy $H(Z|E\Theta)$. The main challenge here is thus

to establish a reliable lower bound on this quantity assuming only the CHSH violation S . More specifically, we are interested in finding a function $C^*(S)$ such that

$$H(Z|E\Theta) \geq C^*(S) \quad (9)$$

holds for *all* possible combinations of states and measurements (in any dimension) that are consistent with the observed CHSH value S . An inequality like equation (9) is commonly referred to as an entropic uncertainty relation, and in our case, we are interested in relations with quantum side-information [22, 37, 38]. There is a vast amount of literature [23, 39, 40] in which relations of this form [22, 37, 38, 41] or similar [42–48] have been studied and several types of uncertainty relations have been discovered. A typical family of entropic uncertainty relation, which is close to our problem, is that proposed by Berta et al. [22] and the weighted generalisation of it from Gao et al. [38]. These inequalities, however, are not device-independent and requires the measurement characterisation of at least one party, which unfortunately is not possible in our setting.

To the best of our knowledge, the only known entropic uncertainty relations for uncharacterised measurements are given by Tomamichel et al. [49] and Lim et al. [15]. There, the uncertainty of the measurement outcomes with side-information is lower bounded by the so-called overlap of the measurements [22], which in turn is further bounded by a function of the CHSH violation. Although these relations are applicable to uncharacterised measurements, they appear fairly weak when applied to our DIQKD proposal, i.e., they do not provide any improvement in the secret key rate when compared to the original protocol.

The lower bound we establish in this work, i.e., the function $C^*(S)$, appears to be optimal, in that it can be saturated by two-qubit states up to numerical precision (see Supplementary Information). $C^*(S)$ is depicted in the right side of Fig. 2 for $\lambda = 0.5$, and in the right side of Fig. 4 for continuous values of λ and $S \in \{2, 2.2, 2.4, 2.6, 2.8, 2\sqrt{2}\}$. On the left side of Fig. 4, we additionally plotted the so-called uncertainty sets [40, 47, 50] of our relation. These are sets that outline all the admissible pairs of entropies $(H(A_0|E), H(A_1|E))$ for a given lower bound on S . We also note that it may seem plausible to independently optimise each term $H(A_0|E)$, $H(A_1|E)$, instead of the sum of them. However, as shown on the right side of Fig. 4, numerical results suggest that optimising the weighted sum of these terms is always better than optimising the individual term: this also highlights where our DIQKD proposal improves over the original protocol.

Computing $C^*(S)$

As mentioned, the complete analysis of our lower bound on $C^*(S)$ is deferred to the Supplementary Information. In the following we will only outline the main steps of the analysis to reduce the computation of $C^*(S)$ to a sequence of problems that can be treated successively. The basic

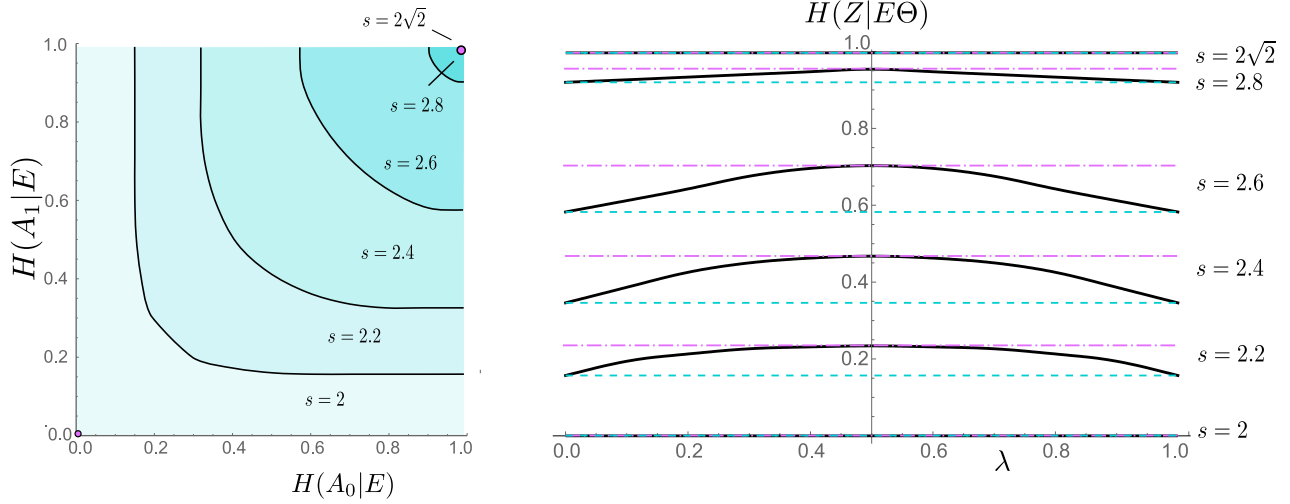


Fig. 4. **Device-independent uncertainty relations:** On the left side, the plot shows the device-independent uncertainty relation between $\lambda H(A_0|E) + (1 - \lambda)H(A_1|E)$, where the solid line is the fundamental uncertainty $C^*(S)$ for a given CHSH violation. The shaded region above the line hence represents the feasible region of $(H(A_0|E), H(A_1|E))$ given S . Evidently, when $S = 2\sqrt{2}$, we see that $H(A_0|E) = H(A_1|E) = 1$ must be maximally random; indeed, $S = 2\sqrt{2}$ corresponds to the case where Eve is completely uncorrelated with the devices and hence her best guess is limited to a random guess. On the right side figure, the plot shows the minimal uncertainty $C^*(S)$ (the bottom dashed line) attained when $\lambda = 0, 1$ and one can see that $C^*(S)$ (solid line) for $0 < \lambda < 1$ always gives a non-trivial advantage over the limiting case (like in the original DIQKD protocol).

idea to find a way to compute $C^*(S)$ by only using known estimates (both analytical and numerical) that give a final lower bound that is reliable. This means that all the steps of the analysis assumes the worst-case scenario, so that final value is a strict lower bound on $C^*(S)$. In brief, the analysis uses a refined version of Pinsker's inequality, semi-definite optimisation and an ε -net to achieve this goal.

Our first step is to reformulate the tripartite problem involving Alice, Bob and Eve to a bipartite one that involves only Alice and Bob. Following Ref. [51], we note that conditional entropy terms like $H(A_0|E)$ can always be reformulated as the entropy production $H(T_X(\rho_{AB})) - H(\rho_{AB})$ of the quantum channel T_X on a complementary system (the post measurement state on the Alice-Bob system). In our case, this channel T_X is a pinching channel, which satisfies $T_X = T_X^2 = T_X^*$ and acts complementary to the map that models Alice's measurement. With this, we can further rewrite the entropy production as

$$\begin{aligned} & \lambda H(A_0|E) + (1 - \lambda)H(A_1|E) \\ &= \lambda H(T_0[\rho_{AB}]) - \lambda H(\rho_{AB}) \\ &+ (1 - \lambda)H(T_1[\rho_{AB}]) - (1 - \lambda)H(\rho_{AB}) \\ &= \lambda D(\rho_{AB} \| T_0[\rho_{AB}]) + (1 - \lambda)D(\rho_{AB} \| T_1[\rho_{AB}]), \end{aligned} \quad (10)$$

where $D(\rho \| \sigma)$ is the quantum relative entropy of ρ with respect to σ .

Then, we follow a proof technique in Ref. [1, 2] to reduce the underlying ρ_{AB} to a mixture of two-qubit states, where it is assumed that the mixing is due to Eve. That is, since each party (Alice and Bob) only perform two binary measurements, their local measurement devices can be described by only specifying two projectors (whose dimensions are unspecified). The corresponding local algebras,

which are generated by two projectors, are well investigated mathematical objects [52] for which a central theorem [53] states that their representation can be decomposed into 2×2 (qubit) blocks and a commuting rest. Correspondingly, this allows us to conclude (details in the Supplementary Information) that desired uncertainty bound can be decomposed accordingly as a convex combination:

$$\begin{aligned} C^*(S) &\geq \inf_{\mu} \int_{S'=2}^{2\sqrt{2}} \mu(dS') C_{\mathbb{C}^{4 \times 4}}^*(S') \quad (11) \\ \text{s.th.: } &\mu([2, 2\sqrt{2}]) \leq 1, \quad \mu \geq 0 \\ &\int_{S'=2}^{2\sqrt{2}} \mu(dS') S' = S, \end{aligned}$$

where $C_{\mathbb{C}^{4 \times 4}}^*(S')$ is a lower bound on the conditional entropy $H(Z|E\Theta)$ for projective measurements on two qubits. Here, we note that once a bound on $C_{\mathbb{C}^{4 \times 4}}^*(S')$ is established, the optimisation over all measures μ , which can be geometrically interpreted as taking a convex hull, is straightforward to perform. As shown in Fig. 5, the situation for the optimisation corresponding to $C_{\mathbb{C}^{4 \times 4}}^*(S')$ can now, w.l.o.g., be fully described by specifying a two-qubit state and two angles (φ, ω) that describe the relative alignment of Alice's and Bob's measurements.

Although the problem has been reduced to two-qubit states and projective qubit measurements, a direct computation of $C_{\mathbb{C}^{4 \times 4}}^*(S')$ is still an open problem as there are no known proof techniques can be applied to our situation. To that end, we employ a refined version of Pinsker's inequality (see Theorem 1 in the Supplementary Information),

$$D(\rho \| T[\rho]) \geq \log(2) - h_2 \left(\frac{1}{2} - \frac{1}{2} \|\rho - T[\rho]\|_1 \right), \quad (12)$$

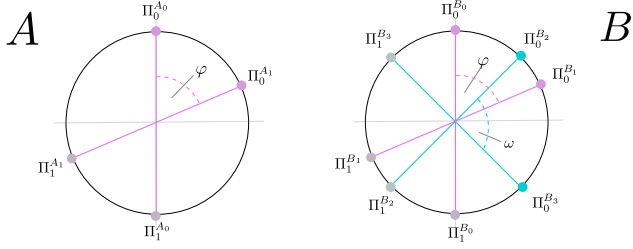


Fig. 5. **Measurement setting for two-qubit states:** Alice has two projective measurement that are described by projectors $(\Pi_0^{A_0}, \Pi_1^{A_0})$ and $(\Pi_0^{A_1}, \Pi_1^{A_1})$ with relative angle φ . Bob has in total four measurements: for key generation, ideally he should perform measurements B_0 and B_1 which are aligned with Alice's measurements A_0 and A_1 to minimise the quantum bit error rates. The security analysis only depends on Bob's measurements B_2 and B_3 , which are w.l.o.g. specified by a relative angle ω .

to obtain a lower bound on the relative entropy in (10) in terms of trace norm.

The big advantage of establishing estimates in terms of trace norm is that a minimisation of trace norm can be formulated as semi-definite program (SDP).

With that, the overall optimisation problem at hand now reads

$$\inf_{\varphi \in [0, \pi/2]} \left(\inf_{\|\mathbf{b}\|_2=1} \left(\inf_{\rho} \lambda \delta(\rho, 0) + (1 - \lambda) \delta(\rho, \varphi) \right) \right) \quad \text{s.t.:} \quad \langle F_0 + \mathbf{F} \cdot \mathbf{b} \rangle_{\rho} = S \quad (13)$$

where

$$\delta(\rho, \varphi) := \left\| \{ \rho, Q(\varphi) \} - 2Q(\varphi)\rho Q(\varphi) \right\|_1 \quad (14)$$

and constraints that are linear in ρ given by 4×4 -matrices

$$F_0 \text{ and } \mathbf{F} \cdot \mathbf{b} = b_x F_x(\varphi) + b_z F_z(\varphi), \quad (15)$$

where $Q(\varphi)$, $F_x(\varphi)$ and $F_y(\varphi)$ depend on φ in terms of the first and second order in $\cos(\varphi)$ and $\sin(\varphi)$. In the above \mathbf{b} is a vector on a (2-norm) unit sphere that arises from reformulating the description of Bob's measurements.

This optimisation can be solved in three stages: indicated by boxes in (13).

- (i) The black box is an SDP on 4×4 matrices, which can be efficiently solved [54].
- (ii) The optimisation in the second box (magenta box) is performed by relaxing the continuous optimisation over the (2-norm) unit sphere to a discrete optimisation on a sequence of polygonal approximation (similar to the method used in Schwonnek et al. [55, 56]). Also this optimisation can be performed with reliable lower bounds to the order of any target precision.
- (iii) The last optimisation in the biggest box (cyan box) only runs over the single parameter φ coming from a bounded domain. Hence, it is possible to efficiently tackle this optimisation by an ε -net. In order to do so it is required to provide an error estimate (for the magenta and the black box) for all φ that are located in ε interval around some φ_0 . Note that all previous optimisations are linear in ρ and \mathbf{b} and only depend in the second order on $\cos(\varphi)$ and $\sin(\varphi)$ (which are bounded functions of φ).

[1] S. Pironio, A. Acín, N. Brunner, N. Gisin, S. Massar, and V. Scarani, *New Journal of Physics* **11**, 045021 (2009).
[2] A. Acín, N. Brunner, N. Gisin, S. Massar, S. Pironio, and V. Scarani, *Physical Review Letters* **98**, 230501 (2007).
[3] J. F. Clauser, M. A. Horne, A. Shimony, and R. A. Holt, *Physical Review Letters* **23**, 880 (1969).
[4] J. S. Bell, *Physics* **1**, 195 (1964).
[5] U. Vazirani and T. Vidick, *Communications of the ACM* **62**, 133 (2019).
[6] R. Arnon-Friedman, R. Renner, and T. Vidick, *SIAM Journal on Computing* **48**, 181 (2019).
[7] U. Vazirani and T. Vidick, in *Proceedings of the 5th conference on Innovations in theoretical computer science* (2014) pp. 35–36.
[8] B. Hensen, H. Bernien, A. E. Dréau, A. Reiserer, N. Kalb, M. S. Blok, J. Ruitenberg, R. F. L. Vermeulen, R. N. Schouten, C. Abellán, W. Amaya, V. Pruneri, M. W. Mitchell, M. Markham, D. J. Twitchen, D. Elkouss, S. Wehner, T. H. Taminiau, and R. Hanson, *Nature* **526**,

682 (2015).
[9] M. Giustina, M. A. M. Versteegh, S. Wengerowsky, J. Handsteiner, A. Hochrainer, K. Phelan, F. Steinlechner, J. Kofler, J.-A. Larsson, C. Abellán, W. Amaya, V. Pruneri, M. W. Mitchell, J. Beyer, T. Gerrits, A. E. Lita, L. K. Shalm, S. W. Nam, T. Scheidl, R. Ursin, B. Wittmann, and A. Zeilinger, *Physical Review Letters* **115**, 250401 (2015).
[10] L. K. Shalm, E. Meyer-Scott, B. G. Christensen, P. Bierhorst, M. A. Wayne, M. J. Stevens, T. Gerrits, S. Glancy, D. R. Hamel, M. S. Allman, K. J. Coakley, S. D. Dyer, C. Hodge, A. E. Lita, V. B. Verma, C. Lambrocco, E. Tortorici, A. L. Migdall, Y. Zhang, D. R. Kumor, W. H. Farr, F. Marsili, M. D. Shaw, J. A. Stern, C. Abellán, W. Amaya, V. Pruneri, T. Jennewein, M. W. Mitchell, P. G. Kwiat, J. C. Bienfang, R. P. Mirin, E. Knill, and S. W. Nam, *Physical Review Letters* **115**, 250402 (2015).
[11] W. Rosenfeld, D. Burchardt, R. Garthoff, K. Redeker, N. Ortegel, M. Rau, and H. Weinfurter, *Physical Review Letters* **119**, 010402 (2017).

- [12] G. Murta, S. B. van Dam, J. Ribeiro, R. Hanson, and S. Wehner, [Quantum Science and Technology](#) **4**, 035011 (2019).
- [13] N. Gisin, S. Pironio, and N. Sangouard, [Physical Review Letters](#) **105**, 070501 (2010).
- [14] M. Curty and T. Moroder, [Phys. Rev. A](#) **84**, 010304 (2011).
- [15] C. C. W. Lim, C. Portmann, M. Tomamichel, R. Renner, and N. Gisin, [Physical Review X](#) **3**, 031006 (2013).
- [16] E. Y.-Z. Tan, C. C.-W. Lim, and R. Renner, [Physical Review Letters](#) **124**, 020502 (2020).
- [17] V. Scarani, H. Bechmann-Pasquinucci, N. J. Cerf, M. Dušek, N. Lütkenhaus, and M. Peev, [Reviews of Modern Physics](#) **81**, 1301 (2009).
- [18] A. Fine, [Journal of Mathematical Physics](#) **23**, 1306 (1982).
- [19] P. Busch, [International Journal of Theoretical Physics](#) **24**, 63 (1985).
- [20] M. M. Wolf, D. Perez-Garcia, and C. Fernandez, [Phys. Rev. Lett.](#) **103**, 230402 (2009).
- [21] R. Horodecki, P. Horodecki, M. Horodecki, and K. Horodecki, [Rev. Mod. Phys.](#) **81**, 865 (2009).
- [22] M. Berta, M. Christandl, R. Colbeck, J. M. Renes, and R. Renner, [Nature Physics](#) **6**, 659 (2010).
- [23] P. Coles, M. Berta, M. Tomamichel, and S. Wehner, [Reviews of Modern Physics](#) **89** (2017), and [arXiv:1511.04857](#).
- [24] D. N. Matsukevich, P. Maunz, D. L. Moehring, S. Olmschenk, and C. Monroe, [Physical Review Letters](#) **100**, 150404 (2008).
- [25] S. Pironio, A. Acín, S. Massar, A. B. de La Giroday, D. N. Matsukevich, P. Maunz, S. Olmschenk, D. Hayes, L. Luo, T. A. Manning, *et al.*, [Nature](#) **464**, 1021 (2010).
- [26] M. Giustina, A. Mech, S. Ramelow, B. Wittmann, J. Kofler, J. Beyer, A. Lita, B. Calkins, T. Gerrits, S. W. Nam, *et al.*, [Nature](#) **497**, 227 (2013).
- [27] B. Christensen, K. McCusker, J. Altepeter, B. Calkins, T. Gerrits, A. E. Lita, A. Miller, L. K. Shalm, Y. Zhang, S. Nam, *et al.*, [Physical Review Letters](#) **111**, 130406 (2013).
- [28] F. Henkel, M. Krug, J. Hofmann, W. Rosenfeld, M. Weber, and H. Weinfurter, [Physical Review Letters](#) **105**, 253001 (2010).
- [29] K. Redeker, Private Communication (2020).
- [30] M. Żukowski, A. Zeilinger, M. A. Horne, and A. K. Ekert, [Physical Review Letters](#) **71**, 4287 (1993).
- [31] P. C. Humphreys, N. Kalb, J. P. Morits, R. N. Schouten, R. F. Vermeulen, D. J. Twitchen, M. Markham, and R. Hanson, [Nature](#) **558**, 268 (2018).
- [32] F. Dupuis, O. Fawzi, and R. Renner, [arXiv:1607.01796](#) (2016).
- [33] R. Arnon-Friedman, F. Dupuis, O. Fawzi, R. Renner, and T. Vidick, [Nature Communications](#) **9**, 459 (2018).
- [34] F. Dupuis and O. Fawzi, [IEEE Transactions on Information Theory](#) **65**, 7596 (2019).
- [35] E. Y.-Z. Tan, R. Schwonnek, K. T. Goh, I. W. Primaatmaja, and C. C.-W. Lim, [arXiv:1908.11372](#) (2019).
- [36] I. Devetak and A. Winter, [Proceedings of the Royal Society A — Mathematical, Physical and Engineering Sciences](#) **461**, 207 (2005).
- [37] R. L. Frank and E. H. Lieb, [Annales Henri Poincaré](#) **13**, 1711 (2012).
- [38] L. Gao, M. Junge, and N. LaRacuente, in *2018 IEEE International Symposium on Information Theory (ISIT)* (2018) pp. 996–1000.
- [39] S. Wehner and A. Winter, [New Journal of Physics](#) **12**, 025009 (2010), [arXiv:0907.3704](#).
- [40] R. Schwonnek, “Uncertainty relations in quantum theory,” (2018), ph.D thesis, Leibniz University Hannover, <https://doi.org/10.15488/3600>.
- [41] S. Liu, L.-Z. Mu, and H. Fan, [Physical Review A](#) **91**, 042133 (2015).
- [42] D. Deutsch, [Physical Review Letters](#) **50**, 631 (1983).
- [43] H. Maassen, *Discrete entropic uncertainty relation* (Springer, 1990) pp. 263–266, ‘Quantum Probability and Applications V’ (Proceedings Heidelberg 1988), Lecture Notes in Mathematics 1442.
- [44] H. Maassen and J. B. Uffink, [Physical Review Letters](#) **60**, 1103 (1988).
- [45] K. Abdelkhalek, R. Schwonnek, H. Maassen, F. Furrer, J. Duhme, P. Raynal, B. Englert, and R. Werner, [Int. J. Quant. Inf.](#) **13**, 1550045 (2015), [arXiv:1509.00398](#).
- [46] J. Schneeloch, C. J. Broadbent, S. P. Walborn, E. G. Cavalcanti, and J. C. Howell, [Physical Review A](#) **87**, 062103 (2013), [arXiv:1303.7432](#).
- [47] R. Schwonnek, [Quantum](#) **2**, 59 (2018).
- [48] A. Riccardi, C. Macchiavello, and L. Maccone, [Physical Review A](#) **95**, 032109 (2017), [arXiv:1701.04304](#).
- [49] M. Tomamichel and E. Hänggi, [Journal of Physics A: Mathematical and Theoretical](#) **46**, 055301 (2013).
- [50] L. Dammeier, R. Schwonnek, and R. Werner, [New Journal of Physics](#) **9**, 093946 (2015), [arXiv:1505.00049](#).
- [51] E. Y.-Z. Tan, R. Schwonnek, K. T. Goh, I. W. Primaatmaja, and C. C.-W. Lim, (2019), [arXiv:1908.11372](#).
- [52] A. Böttcher and I. Spitkovsky, [Linear Algebra and its Applications](#) **432**, 1412 (2010).
- [53] P. R. Halmos, [Transactions of the American Mathematical Society](#) **144**, 381 (1969).
- [54] S. Boyd and L. Vandenberghe, *Convex Optimization* (Cambridge University Press, 2004).
- [55] R. Schwonnek, L. Dammeier, and R. F. Werner, [Physical Review Letters](#) **119**, 170404 (2017).
- [56] Y.-Y. Zhao, G.-Y. Xiang, X.-M. Hu, B.-H. Liu, C.-F. Li, G.-C. Guo, R. Schwonnek, and R. Wolf, [Physical Review Letters](#) **122**, 220401 (2019).

Supplementary information: Robust device-independent quantum key distribution

René Schwonnek,^{1,*} Koon Tong Goh,^{1,*} Ignatius W. Primaatmaja,² Ernest
Y.-Z. Tan,³ Ramona Wolf,⁴ Valerio Scarani,^{2,5} and Charles C.-W. Lim^{1,2}

¹*Department of Electrical & Computer Engineering, National University of Singapore, Singapore*

²*Centre for Quantum Technologies, National University of Singapore, Singapore*

³*Institute for Theoretical Physics, ETH Zürich, Switzerland*

⁴*Institut für Theoretische Physik, Leibniz Universität Hannover, Germany*

⁵*Department of Physics, National University of Singapore, Singapore*

I. SECURITY ANALYSIS

This section documents the derivation of our lower bound on the quantity $C^*(S)$, which is introduced in the main text. $C^*(S)$ is defined as the minimum $H(Z|E\Theta)$ (conditional entropy of Z given side-information $E\Theta$) upon observing a CHSH value of S . Recall that

$$H(Z|E\Theta) := \lambda H(A_0|E) + (1 - \lambda) H(A_1|E) \quad (1)$$

describes Eve's uncertainty about the measurement outcome Z given Θ and is a keystone for determining the secret key rate of our device-independent quantum key distribution (DIQKD) protocols.

Before diving into the derivation, we will furnish the definitions and notations of the quantum states, operators and functionals that will be used throughout this section. In the main text, we considered a Bell scenario where two parties Alice and Bob input measurement settings $X \in \{0, 1\}$ and $Y \in \{0, 1, 2, 3\}$ respectively into their devices and in return, each device outputs a bit. We shall omit the measurement settings $Y = 0, 1$ for the entirety of this section as they do not serve any role in the estimation of $H(Z|E\Theta)$.

Since we are working in a fully device-independent setting, we can assume that all measurements can be written as projectors without any loss of generality (refer to the explanation in [1]). As such, we denote the projectors corresponding to measurements A_0, A_1, B_2, B_3 as

$$A_0 = \{\Pi_0^{A_0}, \Pi_1^{A_0}\}, \quad A_1 = \{\Pi_0^{A_1}, \Pi_1^{A_1}\}, \quad B_2 = \{\Pi_0^{B_2}, \Pi_1^{B_2}\}, \quad \text{and} \quad B_3 = \{\Pi_0^{B_3}, \Pi_1^{B_3}\}, \quad (2)$$

where the subscript of each projector denotes its corresponding measurement outcome. Therefore, the correlation measurement operators are defined by

$$C^{A_0} := \Pi_0^{A_0} - \Pi_1^{A_0}, \quad C^{A_1} := \Pi_0^{A_1} - \Pi_1^{A_1}, \quad C^{B_2} := \Pi_0^{B_2} - \Pi_1^{B_2}, \quad \text{and} \quad C^{B_3} := \Pi_0^{B_3} - \Pi_1^{B_3}. \quad (3)$$

The correlation measurement operators and the correlation function $C_{XY} = P(A_X = B_Y|X, Y) - P(A_X \neq B_Y|X, Y)$ defined in the main text is related via $C_{XY} = \text{tr}(\rho C^{A_X} \otimes C^{B_Y})$ where ρ is the measured quantum state. Hence, the CHSH operator is denoted as

$$CHSH := C^{A_1} \otimes C^{B_2} - C^{A_0} \otimes C^{B_2} - C^{A_0} \otimes C^{B_3} - C^{A_1} \otimes C^{B_3}. \quad (4)$$

Furthermore, we denote the single round quantum state of Alice and Bob by ρ_{AB} and assume that Eve holds the purification of this state. Thus, the joint state describing Alice, Bob, and Eve quantum systems is given by some pure state ψ_{ABE} , whose Hilbert space dimension is unknown. Conventionally, the von Neumann entropy of a quantum state ρ is denoted and defined by $H(\rho) := -\text{tr}(\rho \log \rho)$, we shall adopt the shorthand notation of

$$H(AB) = H(\rho_{AB}), \quad H(B) = H(\rho_B), \quad H(E) = H(\rho_E) \dots \quad (5)$$

to denote the entropy of a specific subsystem, whenever the underlying state is clear from the context. Next, a classical-quantum state after the action of Alice's measurement, A_X , is modelled by

$$\rho_{A_X B E} = \sum_{i \in \{0, 1\}} |i\rangle\langle i| \otimes \text{tr}_A \left((\Pi_i^{A_X} \otimes \mathbf{1}_{BE}) \psi_{ABE} (\Pi_i^{A_X} \otimes \mathbf{1}_{BE}) \right), \quad (6)$$

* These authors contributed equally to this work.

where $|i\rangle\langle i|$ indexes a classical register that stores the measurement outcomes. Thus, the conditional entropy $H(A_X|E) = H(A_X E) - H(E)$ is well-defined for any given joint quantum state describing Alice, Bob and Eve's systems through the above-mentioned relations.

Finally, we could state the proper mathematical definition of $C^*(S)$ using the furnished definitions:

$$C^*(S) = \inf_{A_0, A_1, B_2, B_3} \inf_{\psi_{ABE}} \lambda H(A_0|E) + (1 - \lambda) H(A_1|E) \quad \text{s.t.:} \quad \langle CHSH \rangle_{\rho_{AB}} = S. \quad (7)$$

In the following subsections, we will provide the detailed derivation of our lower bound on the quantity $C^*(S)$ and the structure of the proceedings are organised as follows:

- IA We start by following a well-known argument [1–3], which allows us to reformulate the estimation of conditional entropy of Eve in a tripartite scenario into the estimation of **entropy production on the Alice-Bob system**.
- IB We proceed by following the argument of Pironio et al.[4], which allows us to conclude that the worst case, i.e. the optimal attack of Eve, can always be realised by Alice and Bob performing a convex combination of **projective measurements on a two qubit state**. Even though the problem now may seem straightforward, it still requires the application of a suite of non-trivial numerical and analytical methods. This is due to the fact that the simultaneous optimisation over states and measurements is neither linear nor convex.
- IC We then apply a new refined version of Pinsker's inequality (see Thm. 1) that enables the estimation of entropies via certain trace norms. The remaining problem of **optimising over trace norms** can then be bounded using an efficient algorithm, which will be introduced in the follow subsections.
- ID We first **formulate the optimisation over the unknown quantum state as a semi-definite program (SDP)**.
- IE Although the **optimisation over Bob's measurements** is not convex, we formulated an efficient algorithm that lower bounds this optimisation up to arbitrary precision.
- IF At this stage, it only remains to **optimise over Alice's measurements**. Similar to the previous subsection, optimising over Alice's measurements also result in a non-convex optimisation problem. Since this optimisation only involves a single parameter, which is the angle φ between Alice's measurements, we could simply employ an adaptive refining ε -net. This is possible as all operators involved in the previous steps can be explicitly bounded in norm.
- IG At this point we are able to compute reliable and arbitrarily tight lower bounds on $C^*(S)$ for any two-qubit strategy. Using IB, we are able to compute the final $C^*(S)$ for a raster of different Bell violations S on qubits and taking its convex hull subsequently.

A. Reduction to locally accessible quantities

The defining advantage of quantum over classical cryptography stems from the fact that for a quantum system it is possible to witness the action of Eve, given only access to the Alice-Bob subsystem. In this subsection, we will relate the conditional entropy $H(A_X|E)$, which depends on Eve's system, to quantities that only depends on Alice and Bob's systems. Such effort will allow us to circumvent the obstacle of having to perform optimisation over Eve's quantum system with unbounded Hilbert space dimension.

We begin by viewing any key generating measurement, A_X , of the DIQKD protocol from the perspective of a larger Hilbert space (similarly to the appendix of [2]) by introducing a classical memory \mathcal{A}_X that is used to store the measurement outcome. We denote \mathcal{A}_X^{init} as the abelian algebra describing the initial (empty) state of the memory and ϕ as its associated pure quantum state. As such, the process of measuring A_X on Alice's quantum system (modelled by von Neumann algebra \mathcal{A}) and recording the outcome into the memory can be described by a unitary evolution that transforms the pure initial state $\Psi_{ABE} \otimes \phi$ into a final state $\Psi_{A'BEA_X}$. Note that the unitary evolution also involves the transformation of \mathcal{A} into the post measurement state of a system \mathcal{A}' . Hence, $H(A_X|E)$ can be understood as entropy production ΔH on the memory-Eve system.

From the dilated perspective (see Fig. 1), the memory-Eve system is only one side of a bipartition, where the Alice-Bob system is the other. Since the local von Neumann entropies on two sides of a bipartite pure state are equal (see Thm.2(c) of [5]), the entropy production on the Alice-Bob system is equal to the entropy production of the memory-Eve system. Consequently, we can conclude that

$$H(A_X|E) = H(A_X E) - H(E) = H(A_X E) - H(A_X^{init} E) \quad (8)$$

$$= H(A'B) - H(AB) := \Delta H \quad (9)$$

$$\Psi_{ABE} \otimes \phi \xrightarrow{\text{measurement}} \Psi_{A'BEA_X}$$

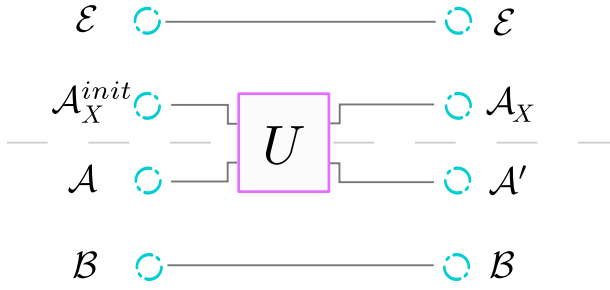


Fig. 1. **The Stinespring dilated perspective:** A key generating measurement A_X is regarded from the perspective of a higher Hilbert space by including the action $A_X \rightarrow A_X^{init}$ on a classical memory (an abelian algebra). From this perspective the global state before and after the measurement is pure. In this case, due to the Araki-Lieb inequality (see Thm.2(c) of [5]), the entropy production $\Delta H = H(A_X|E)$ on the Eve-Memory partition equals the entropy change on the Alice-Bob partition. This allows us to bound $H(A_X|E)$ by measuring only on the Alice-Bob partition, i.e. without accessing Eve's system.

Therefore, we could restrict the values of $H(A_X|E)$ by only considering the transformation $\mathcal{AB} \rightarrow \mathcal{A}'\mathcal{B}$. A short calculation (see [1–3]) shows that this transformation is described by the pinching channels, defined by

$$\begin{aligned} T_0[\rho] &:= (\Pi_0^{A_0} \otimes \mathbf{1}) \rho (\Pi_0^{A_0} \otimes \mathbf{1}) + (\Pi_1^{A_0} \otimes \mathbf{1}) \rho (\Pi_1^{A_0} \otimes \mathbf{1}) \\ T_1[\rho] &:= (\Pi_0^{A_1} \otimes \mathbf{1}) \rho (\Pi_0^{A_1} \otimes \mathbf{1}) + (\Pi_1^{A_1} \otimes \mathbf{1}) \rho (\Pi_1^{A_1} \otimes \mathbf{1}). \end{aligned} \quad (10)$$

Following the definitions of the pinching channels, we have the identities $T[\rho] = T \circ T[\rho] = T^*[\rho]$ and also $f(T[\rho]) = T[f(T[\rho])]$ when used within a functional calculus for a measurable function f . Hence, we can conclude that:

$$\begin{aligned} H(T[\rho]) - H(\rho) &= -\text{tr}(T[\rho] \log(T[\rho])) + \text{tr}(\rho \log(\rho)) \\ &= -\text{tr}(\rho T^*[\log(T[\rho])]) + \text{tr}(\rho \log(\rho)) \\ &= -\text{tr}(\rho \log(T[\rho])) + \text{tr}(\rho \log(\rho)) \\ &= D(\rho \| T[\rho]), \end{aligned} \quad (11)$$

where $D(\rho \| \sigma)$ denotes the relative entropy. Therefore, we can rewrite the convex mixture of conditional entropies as

$$\begin{aligned} &\lambda H(A_0|E) + (1 - \lambda) H(A_1|E) \\ &= \lambda H(T_0[\rho_{AB}]) - \lambda H(\rho_{AB}) + (1 - \lambda) H(T_1[\rho_{AB}]) - (1 - \lambda) H(\rho_{AB}) \\ &= \lambda D(\rho_{AB} \| T_0[\rho_{AB}]) + (1 - \lambda) D(\rho_{AB} \| T_1[\rho_{AB}]) \end{aligned} \quad (12)$$

Thus, we are able to bound Eve's conditional uncertainty on the measurement outcomes from any convex mixture of measurement bases by estimating the entropy production on the Alice-Bob system.

B. Restriction to qubits

In this subsection, we will show that for the purpose of bounding $C^*(S)$, we could without loss of generality consider Alice-Bob system as a convex combination of two-qubits states.

A fundamental theorem on the algebra generated by a pair of two projections [6–9], which will be in our case $(\Pi_0^{A_0}, \Pi_0^{A_1})$ such as $(\Pi_0^{B_2}, \Pi_0^{B_3})$, states that we can always find a representation of the respective system of Alice and Bob that allows us to decompose the projectors into 2×2 blocks and a commuting rest.

In particular, let K^A, L^A, K^B and L^B be pairwise commuting projectors and let

$$Q(\theta) = \begin{pmatrix} \cos(\theta/2)^2 & \cos(\theta/2) \sin(\theta/2) \\ \cos(\theta/2) \sin(\theta/2) & \sin(\theta/2)^2 \end{pmatrix} \quad (13)$$

be a family of 2×2 projectors. Then, we can decompose

$$\Pi_0^{A_0} = \bigoplus_j \begin{pmatrix} 1 & 0 \\ 0 & 0 \end{pmatrix} \oplus K^A \text{ and } \Pi_0^{A_1} = \bigoplus_j Q(\varphi_j) \oplus L^A \quad (14)$$

$$\Pi_0^{B_2} = \bigoplus_l \begin{pmatrix} 1 & 0 \\ 0 & 0 \end{pmatrix} \oplus K^B \text{ and } \Pi_0^{B_3} = \bigoplus_l Q(\omega_l) \oplus L^B \quad (15)$$

where $\{\varphi_j\}$ and $\{\omega_l\}$ are families of angles that can be obtained from the spectra of $\sigma(\Pi_0^{A_0} + \Pi_0^{A_1})$ and $\sigma(\Pi_0^{B_2} + \Pi_0^{B_3})$ respectively (see [9] for details). The representations of the remaining projectors $\Pi_1^{A_0}, \Pi_1^{A_1}, \Pi_1^{B_2}$ and $\Pi_1^{B_3}$ follow from the identities

$$\Pi_1^{A_x} = \mathbf{1} - \Pi_0^{A_x} \text{ and } \Pi_1^{B_y} = \mathbf{1} - \Pi_0^{B_y}. \quad (16)$$

Furthermore, we can also always find channels T_{block}^A, T_{block}^B and $T_{block}^{AB} := T_{block}^A \otimes T_{block}^B$ that diagonalise the entire systems of Alice and Bob into the corresponding blocks of (14) and (15). Applying these channels on an arbitrary state ρ_{AB} will therefore give us a corresponding decomposition

$$T_{block}^{AB}[\rho_{AB}] = \bigoplus_{jl} \mu_{jl} \rho^{jl} \oplus \mu_{rest} \sigma_{rest}, \quad (17)$$

where σ_{rest} denotes the projection of ρ_{AB} into blocks that are commuting on either Alice's and/or Bob's side while the coefficients μ_{jl} can be obtained by renormalising $T_{block}^{AB}[\rho_{AB}]$ blockwise (see [4]). As the pinching channels T_0 and T_1 commute with T_{block}^{AB} by construction and by using data processing, we can estimate

$$\begin{aligned} & \lambda D(\rho_{AB} \| T_0[\rho_{AB}]) + (1 - \lambda) D(\rho_{AB} \| T_1[\rho_{AB}]) \\ & \geq \lambda D(T_{block}^{AB}[\rho_{AB}] \| T_0 \circ T_{block}^{AB}[\rho_{AB}]) + (1 - \lambda) D(T_{block}^{AB}[\rho_{AB}] \| T_1 \circ T_{block}^{AB}[\rho_{AB}]) \\ & = \sum_{jl} \mu_{jl} \left(\lambda D(\rho_{AB}^{jl} \| T_0[\rho_{AB}^{jl}]) + (1 - \lambda) D(\rho_{AB}^{jl} \| T_1[\rho_{AB}^{jl}]) \right) + \mu_{rest} (\lambda D(\sigma_{rest} \| T_0[\sigma_{rest}]) + (1 - \lambda) D(\sigma_{rest} \| T_1[\sigma_{rest}])). \end{aligned} \quad (18)$$

Relating back to the constraint of optimisation (7), we have $CHSH = T_{block}^{AB}[CHSH]$ which implies

$$\text{tr}(\rho_{AB} CHSH) = S \Leftrightarrow \text{tr}(\rho_{AB}^{jl} CHSH) = S^{jl} \text{ and } \sum_{jl} \mu_{jl} S^{jl} = S, \quad (19)$$

where we already took into account that σ_{rest} will not play any role in the following optimisation as $|\text{tr}(\sigma_{rest} CHSH)| \leq 2$ since the corresponding blocks commute on at least one side. Using the above relations, we can optimise every ρ_{AB}^{jl} individually and reformulate (7) as

$$C^*(S) = \inf_{A_0, A_1, B_2, B_3} \inf_{\substack{\{\mu_{jl}\} \\ \sum_{jl} \mu_{jl} \leq 1}} \inf_{\substack{\{S^{jl}\} \\ \sum_{jl} \mu_{jl} S^{jl} = S}} \sum_{jl} \mu_{jl} \begin{aligned} & \inf_{\rho_{AB}^{jl}} \lambda D(\rho_{AB}^{jl} \| T_0[\rho_{AB}^{jl}]) + (1 - \lambda) D(\rho_{AB}^{jl} \| T_1[\rho_{AB}^{jl}]) \\ & \text{s.th.: } \langle CHSH \rangle_{\rho_{AB}^{jl}} = S^{jl} \end{aligned} \quad (20)$$

In the above we lower bound $\inf_{\rho_{AB}^{jl}}[\dots]$ by the function

$$C_{\mathbb{C}^{4 \times 4}}^*(s) = \inf_{\varphi, \omega} \inf_{\substack{\rho_{AB}^{jl} \\ \text{s.th.: } \langle CHSH \rangle_{\rho_{AB}^{jl}} = s}} \lambda D(\rho_{AB}^{jl} \| T_0[\rho_{AB}^{jl}]) + (1 - \lambda) D(\rho_{AB}^{jl} \| T_1[\rho_{AB}^{jl}]) \quad (21)$$

Since (21) is by construction independent of the specific angles of the underlying measurements A_0, A_1, B_2, B_3 , we can reduce the optimisation over all measurements A_0, A_1, B_2, B_3 to an optimisation over all possible $\{\mu_{jl}\}$. Hence we can conclude the bound

$$\begin{aligned} C^*(s) & \geq \inf_{A_0, A_1, B_2, B_3} \inf_{\substack{\{\mu_{jl}\} \\ \sum_{jl} \mu_{jl} \leq 1}} \inf_{\substack{\{S^{jl}\} \\ \sum_{jl} \mu_{jl} S^{jl} = s}} \sum_{jl} \mu_{jl} C_{\mathbb{C}^{4 \times 4}}^*(S^{jl}) \\ & \geq \inf_{\mu} \int_{S'=2}^{2\sqrt{2}} \mu(dS') C_{\mathbb{C}^{4 \times 4}}^*(S') \\ & \text{s.th.: } \mu([2, 2\sqrt{2}]) \leq 1, \quad \mu \geq 0, \quad \int_{S'=2}^{2\sqrt{2}} \mu(dS') S' = S, \end{aligned} \quad (22)$$

by estimating the optimisation over all $\{\mu_{jl}\}$ of arbitrary length via an integral over a positive sub-normalised measure μ . The boundaries of the above integration originate from the simple observation that S can not be larger than $2\sqrt{2}$ and that $C_{\mathbb{C}^{4 \times 4}}^*(S^{jl}) = 0$ for all $S \leq 2$, which in fact also gives us the justification to ignore the σ_{rest} contribution in (18).

At this point, we can write down an explicit matrix representation of the CHSH operator. For reasons that will be clear in the following steps, it is convenient to decompose the CHSH operator with respect to Bob measurements as

$$CHSH = F_0 + b_x F_x + b_z F_z \quad (23)$$

with

$$\begin{aligned} b_x &= \sin(\omega) & b_z &= \cos(\omega) \\ F_0 &= \begin{pmatrix} \cos(\varphi) - 1 & 0 & -\sin(\varphi) & 0 \\ 0 & 1 - \cos(\varphi) & 0 & \sin(\varphi) \\ -\sin(\varphi) & 0 & 1 - \cos(\varphi) & 0 \\ 0 & \sin(\varphi) & 0 & \cos(\varphi) - 1 \end{pmatrix} \\ F_x &= \begin{pmatrix} 0 & 2\cos^2\left(\frac{\varphi}{2}\right) & 0 & -\sin(\varphi) \\ 2\cos^2\left(\frac{\varphi}{2}\right) & 0 & -\sin(\varphi) & 0 \\ 0 & -\sin(\varphi) & 0 & -2\cos^2\left(\frac{\varphi}{2}\right) \\ -\sin(\varphi) & 0 & -2\cos^2\left(\frac{\varphi}{2}\right) & 0 \end{pmatrix} \\ F_z &= \begin{pmatrix} -\cos(\varphi) - 1 & 0 & \sin(\varphi) & 0 \\ 0 & \cos(\varphi) + 1 & 0 & -\sin(\varphi) \\ \sin(\varphi) & 0 & \cos(\varphi) + 1 & 0 \\ 0 & -\sin(\varphi) & 0 & -\cos(\varphi) - 1 \end{pmatrix} \end{aligned} \quad (24)$$

and reformulate the optimisation over Bob's angle ω as an optimisation over two parameters b_x, b_z fulfilling the constraint $b_x^2 + b_z^2 = 1$. Hence our optimisation problem for a single two-qubit state reads

$$C_{\mathbb{C}^{4 \times 4}}^*(S) := \inf_{\varphi \in [0, \pi/2]} \inf_{\substack{(b_x, b_z) \\ b_x^2 + b_z^2 = 1}} \inf_{\rho} \lambda D(\rho \| T_0[\rho]) + (1 - \lambda) D(\rho \| T_1[\rho]) \quad \text{s.th.:} \quad \langle F_0 \rangle_{\rho} + b_x \langle F_x \rangle_{\rho} + b_z \langle F_z \rangle_{\rho} = S, \quad (25)$$

where we will, with a slight abuse of notation, denote the pinching channels for the reduced 2×2 measurements as T_0 and T_1 as well.

C. Estimating the relative entropy via the trace norm (Pinsker++)

In this subsection, we will show that a lower bound of $C_{\mathbb{C}^{4 \times 4}}^*(S)$ is related to an optimisation with its objective function given by a combination of trace norms. As such, this optimisation can be efficiently bounded as shown in the following subsections. Here, we employ a refined version of Pinsker's inequality provided in Theorem 1 (also see [10]): for a pinching channel with two-outcomes we can lower bound the relative entropy between its input and output by their trace norm via

$$D(\rho \| T_X[\rho]) \geq \log(2) - h_2\left(\frac{1}{2} - \frac{1}{2} \|\rho - T_X[\rho]\|_1\right), \quad (26)$$

where $h_2(p) = -p \log p - (1 - p) \log(1 - p)$ denotes the binary entropy function. Using the above inequality and the concavity of the binary entropy, we could write

$$\begin{aligned} & \lambda D(\rho \| T_0[\rho]) + (1 - \lambda) D(\rho \| T_1[\rho]) \\ & \geq \log(2) - \lambda h_2\left(\frac{1}{2} - \frac{1}{2} \|\rho - T_0[\rho]\|_1\right) - (1 - \lambda) h_2\left(\frac{1}{2} - \frac{1}{2} \|\rho - T_1[\rho]\|_1\right) \\ & \geq \log(2) - h_2\left(\frac{1}{2} - \frac{1}{2} \left(\lambda \|\rho - T_0[\rho]\|_1 + (1 - \lambda) \|\rho - T_1[\rho]\|_1\right)\right) \end{aligned} \quad (27)$$

which is a monotonous function of the sum of the trace norms. Hence, we can employ the inequality

$$C_{\mathbb{C}^{4 \times 4}}^*(S) \geq \log(2) - h_2\left(\frac{1}{2} - \frac{1}{2} t\right) \quad (28)$$

for any $t \leq t^*(S)$ that gives a lower bound on the optimisation

$$t^*(S) := \inf_{\varphi \in [0, \pi/2]} \inf_{\substack{(b_x, b_z) \\ b_x^2 + b_z^2 = 1}} \inf_{\rho} \begin{cases} \lambda \|\rho - T_0[\rho]\|_1 + (1 - \lambda) \|\rho - T_1[\rho]\|_1 \\ \text{s.th.: } \langle F_0 \rangle_{\rho} + b_x \langle F_x \rangle_{\rho} + b_z \langle F_z \rangle_{\rho} = S \end{cases} \quad (29)$$

The boxes in (29) highlight different stages in the optimisation that will be addressed individually in the following three subsections.

D. Optimisation of ρ for fixed angles: reformulation as SDP

In this subsection, we will formulate the minimisation over ρ (black box in (29)) as a SDP, which can be solved using existing numerical algorithms. To this end, we will use a well-known relation that the trace norm of a quadratic matrix V can be represented by the minimisation (refer to [11])

$$\|V\|_1 = \inf_{K, L} \frac{1}{2} \text{tr}(K + L) \quad \text{s.th.:} \begin{pmatrix} K & V \\ V^\dagger & L \end{pmatrix} \geq 0. \quad (30)$$

over additional matrices K and L . We can explicitly expand the channels T_X in terms of the measurement projectors, which can be written as

$$\rho - T_1(\rho) = \rho Q(\varphi) + Q(\varphi)\rho - 2Q(\varphi)\rho Q(\varphi) \text{ and } \rho - T_0(\rho) = \rho Q(0) + Q(0)\rho - 2Q(0)\rho Q(0). \quad (31)$$

Hence, we can rewrite the minimisation over ρ as the following SDP:

$$\begin{aligned} & \boxed{\begin{aligned} & \inf_{\rho} \quad \lambda \|\rho - T_0[\rho]\|_1 + (1 - \lambda) \|\rho - T_1[\rho]\|_1 \\ & \text{s.th.: } \langle F_0 \rangle_{\rho} + b_x \langle F_x \rangle_{\rho} + b_z \langle F_z \rangle_{\rho} = S \end{aligned}} \\ &= \inf_{\substack{\rho \\ K_0, L_0, K_1, L_1}} \lambda \text{tr}(K_0 + L_0) + (1 - \lambda) \text{tr}(K_1 + L_1) \\ & \quad \text{s.th.:} \quad \begin{pmatrix} K_0 & \rho Q(0) + Q(0)\rho - 2Q(0)\rho Q(0) \\ \rho Q(0) + Q(0)\rho - 2Q(0)\rho Q(0) & L_0 \end{pmatrix} \geq 0 \\ & \quad \begin{pmatrix} K_1 & \rho Q(\varphi) + Q(\varphi)\rho - 2Q(\varphi)\rho Q(\varphi) \\ \rho Q(\varphi) + Q(\varphi)\rho - 2Q(\varphi)\rho Q(\varphi) & L_1 \end{pmatrix} \geq 0 \\ & \quad \text{tr}(\rho(F_0 + b_x F_x + b_z F_z)) = S. \end{aligned} \quad (32)$$

$$\begin{aligned} & \text{tr}(\rho(F_0 + b_x F_x + b_z F_z)) = S. \end{aligned} \quad (33)$$

E. Optimisation of Bob's angle: an outer approximation to b_x, b_z

The minimisation over Bob's measurement angle (the magenta box in (29)) was formulated as an optimisation over parameters (b_x, b_z) from a set

$$\mathcal{K} = \{(b_x, b_z) | b_x^2 + b_z^2 = 1\}, \quad (34)$$

which can be interpreted as boundary of a circle with unit radius. Since the objective function of (29) does not explicitly depends on (b_x, b_z) , we could move this minimisation directly into the constraints and write

$$\inf_{\substack{b_x, b_z \\ b_x^2 + b_z^2 = 1}} \left[\begin{array}{l} \inf_{\rho} \quad \lambda \|\rho - T_0[\rho]\|_1 + (1 - \lambda) \|\rho - T_1[\rho]\|_1 \\ \text{s.th.: } \langle F_0 \rangle_{\rho} + b_x \langle F_x \rangle_{\rho} + b_z \langle F_z \rangle_{\rho} = S \end{array} \right] \quad (35)$$

$$= \inf_{\rho} \quad \lambda \|\rho - T_0[\rho]\|_1 + (1 - \lambda) \|\rho - T_1[\rho]\|_1 \\ \text{s.th.: } \exists (b_x, b_z) \in \mathcal{K} : \quad \langle F_0 \rangle_{\rho} + b_x \langle F_x \rangle_{\rho} + b_z \langle F_z \rangle_{\rho} = S \quad (36)$$

$$= \inf_{\rho} \quad \lambda \|\rho - T_0[\rho]\|_1 + (1 - \lambda) \|\rho - T_1[\rho]\|_1 \\ \text{s.th.: } \sup_{(b_x, b_z) \in \mathcal{K}} \langle F_0 \rangle_{\rho} + b_x \langle F_x \rangle_{\rho} + b_z \langle F_z \rangle_{\rho} \geq S. \quad (37)$$

Clearly, the above problem is no longer a convex optimisation problem but there exists a convex relaxation by replacing \mathcal{K} with any convex set $\mathcal{P} \supseteq \mathcal{K}$. We will replace \mathcal{K} by a compact convex polytope \mathcal{P} with finite set of vertices (p_x^l, p_z^l) . Since the individual constraints in (35) are linear in b_x, b_z , it suffices to only consider points on these vertices. As such, we can efficiently lower bound (35) via

$$(35) \geq \inf_{\rho} \quad \lambda \|\rho - T_0[\rho]\|_1 + (1 - \lambda) \|\rho - T_1[\rho]\|_1 \\ \text{s.th.: } \sup_{(b_x, b_z) \in \mathcal{P}} \langle F_0 \rangle_{\rho} + b_x \langle F_x \rangle_{\rho} + b_z \langle F_z \rangle_{\rho} \geq S \geq \inf_l \inf_{\rho} \quad \lambda \|\rho - T_0[\rho]\|_1 + (1 - \lambda) \|\rho - T_1[\rho]\|_1 \\ \text{s.th.: } \langle F_0 \rangle_{\rho} + p_x^l \langle F_x \rangle_{\rho} + p_z^l \langle F_z \rangle_{\rho} \geq S \quad (38)$$

The above structure can now be incorporated in a simple algorithm (illustrated in Fig. 2) that computes the optimisation of Bob's measurements via a sequence of lower bounds (also see [12, 13] where a similar method was used for 3-dimensional problems). The algorithm is given by:

- (i) Start by initiating \mathcal{P} as a rectangle that contains \mathcal{K} .
- (ii) Use (32) to compute the value of (38) for every vertices $(p_x^1, p_z^1) \dots (p_x^n, p_z^n)$ of \mathcal{P} .
- (iii) Pick the first vertex b_{min} that attains the minimum in (38) and refine \mathcal{P} by introducing a new edge to \mathcal{P} that is tangential to \mathcal{K} . This will "cut off" b_{min} and create two new vertices (see Fig.2). Proceed to (ii).

Repeating (ii) and (iii) will give a progressive refinement of \mathcal{P} that approaches the boundary of \mathcal{K} from the outside at the vicinity of those points (b_x, b_z) that realise the minimum of (29). It turns out that, this algorithm only requires a few iterations to achieve a very high precision for our above-mentioned problem.

F. Optimisation of Alice's angle: an ε -net for φ

For the representation given by equation (14), Alice's measurement on her qubit is fully described by the angle φ , which could take values in the interval $[0, \pi/2]$. Consequently, the minimisation over Alice's measurement angle (cyan box in (29)) is not a SDP.

In this subsection, we will show how one could obtain a bound on the minimisation over Alice's measurement angle by employing an ε -net. The basic idea of the ε -net is as follows: we split the interval $[0, \pi/2]$ into smaller segments of size $2\varepsilon_0$ each centred around a raster-point φ_i . We then evaluate (29) (i.e. everything in the magenta box) on each raster-point and subtract a pessimistic error $\Delta(\varepsilon_0, \varphi)$, which bounds how much would the value of (29) have changed when evaluated on any other φ within the segment. Taking the minimal value over all segments will then give us a lower bound on the whole optimisation (29)(cyan box).

Refining those segments into even smaller ones will give tighter lower bounds. In order to keep the total computational cost low, we successively refine only the segment that gives the minimum value for a given round of the procedure. By doing so, we arrive in a situation (see Fig.3) where we only have to improve our refinement around a single point corresponding to the global minimum, i.e. the single φ that achieves $C_{\mathbb{C}^{4 \times 4}}^*(S)$.

In order to bound the error of each segment, we will need to investigate the relation between the entire optimisation and Alice's measurement angle φ . Varying φ (see (14)) will affect the two inner optimisations of (29) in two ways: On

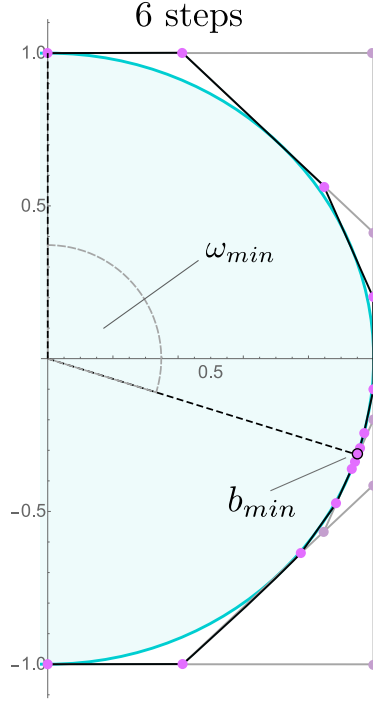
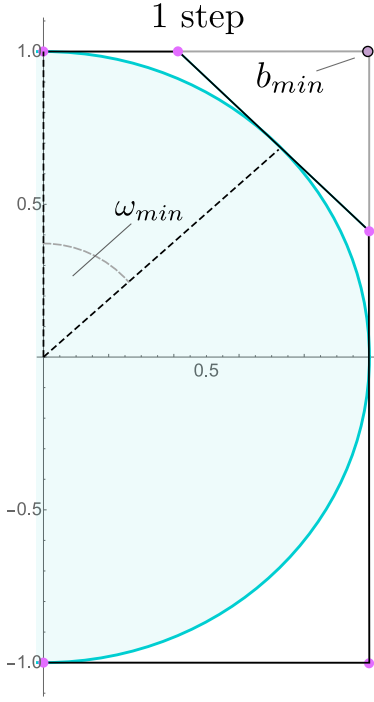


Fig. 2. **Minimising ω :** Iterative refinement of \mathcal{P} (magenta vertices, black edges) to identify the optimal ω in \mathcal{K} (cyan semicircle). The parameters considered in the diagram is given by $\lambda = 0.2$, $S = 2.4$ and $\varphi = 1.2$. In every iteration of our algorithm, we identify b_{min} (grey circles), the vertex of \mathcal{P} that gives the minimum value of optimisation (38), and remove it by introducing a new edge. In this example, six iterations are sufficient to achieve a target precision of 10^{-5} .

one hand, since the objective function depends on φ via the $T_1(\rho)$, it will change with varying φ . On the other hand, the feasible set of possible ρ_{AB} will change with varying φ since the CHSH operator, i.e. F_0, F_x and F_z , depends on φ as well.

We will now address the dependence of the CHSH operator on φ . Without loss of generality we could have reformulated (29) by considering all states that could achieve a Bell violation *greater* than or equals the observed CHSH value S as it is a valid relaxation of the optimisation problem. This implies that for fixed φ we could also perform our optimisation over the set

$$\mathcal{S}_\varphi^S := \{\rho | \langle CHSH \rangle_\rho \geq S\}. \quad (39)$$

When we change φ to $\varphi + \varepsilon$, on a segment specified by $|\varepsilon| \leq \varepsilon_0$, we have to consider a different set of states $\mathcal{S}_{\varphi+\varepsilon}^S$. Hence, the optimal solution on the whole segment around φ will be attained on a state from the set

$$\overline{\mathcal{S}}_{\varepsilon_0\varphi}^S := \bigcup_{|\varepsilon| \leq \varepsilon_0} \mathcal{S}_{\varphi+\varepsilon}^S \quad (40)$$

We consider the norm of the difference of the two CHSH operators and we have:

$$\begin{aligned} & \|CHSH|_\varphi - CHSH|_{\varphi-\varepsilon}\|_\infty \\ &= \|(F_0 + b_x F_x + b_z F_z)|_\varphi - (F_0 + b_x F_x + b_z F_z)|_{\varphi-\varepsilon}\|_\infty \\ &= 2\|(Q(\varphi) - Q(\varphi - \varepsilon)) \otimes (C^{B_2} + C^{B_3})\|_\infty \\ &\leq 4\|Q(\varphi) - Q(\varphi - \varepsilon)\|_\infty \\ &\leq 4 \max_{\varphi, |\varepsilon| \leq \varepsilon_0} \|Q(\varphi) - Q(\varphi - \varepsilon)\|_\infty \end{aligned} \quad (41)$$

$$= 4 \max_{\varphi, |\varepsilon| \leq \varepsilon_0} \left\| \begin{pmatrix} \cos(\frac{\varphi}{2})^2 - \cos(\frac{\varphi-\varepsilon}{2})^2 & \cos(\frac{\varphi}{2}) \sin(\frac{\varphi}{2}) - \cos(\frac{\varphi-\varepsilon}{2}) \sin(\frac{\varphi-\varepsilon}{2}) \\ \cos(\frac{\varphi}{2}) \sin(\frac{\varphi}{2}) - \cos(\frac{\varphi-\varepsilon}{2}) \sin(\frac{\varphi-\varepsilon}{2}) & \sin(\frac{\varphi}{2})^2 - \sin(\frac{\varphi-\varepsilon}{2})^2 \end{pmatrix} \right\|_\infty \quad (42)$$

$$= 4 \max_{|\varepsilon| \leq \varepsilon_0} \sqrt{\frac{1}{2} - \frac{1}{2} \cos(\varepsilon)} \quad (43)$$

$$\leq 2\varepsilon_0, \quad (44)$$

where we assumed that $b_x^2 + b_z^2 = 1$ holds up to a negligible deviation (otherwise, adding a further factor $\approx 1 + \epsilon$ will be required). From the above relation, we conclude that every state ρ that could attain a CHSH value S for measurements with the measurement angle $\varphi + \varepsilon$ will attain a CHSH value of at least $S - 2\varepsilon_0$ with the measurements angle φ . Hence, we have the inclusion relation:

$$\overline{\mathcal{S}}_{\varepsilon_0\varphi}^S \subseteq \mathcal{S}_\varphi^{S-2\varepsilon_0}. \quad (45)$$

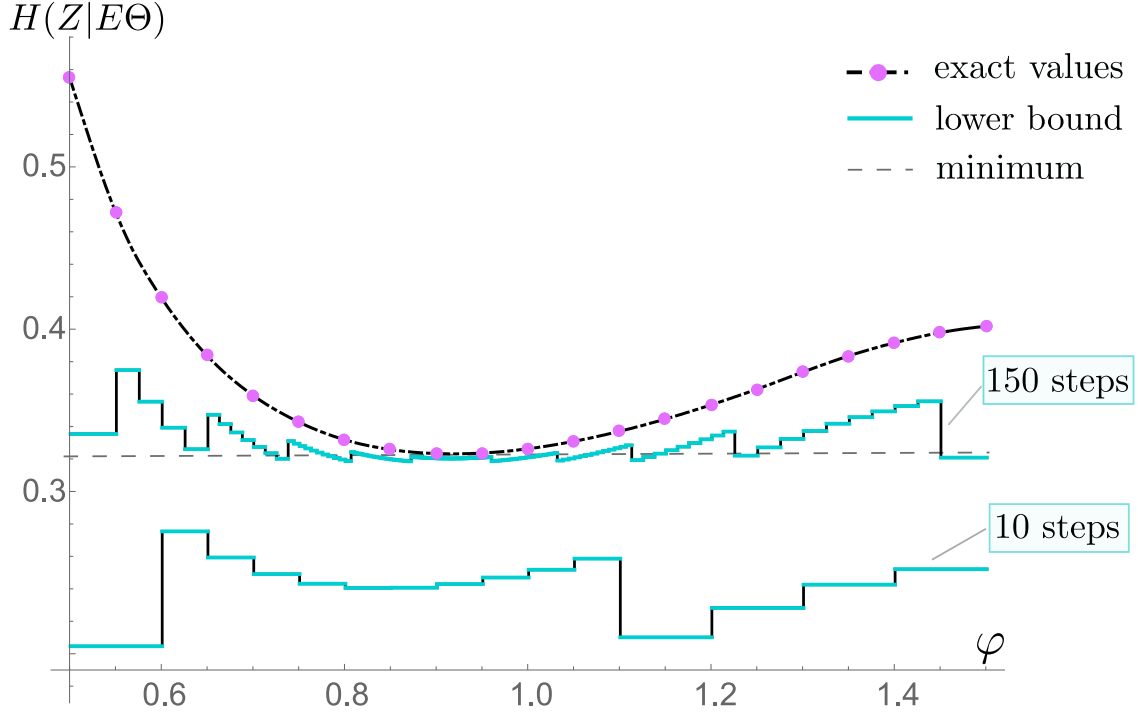


Fig. 3. **Adaptive refinement of the ε -net** Lower bounds on $H(Z|E\theta)$, by evaluating (28) on segments. (For comparison) The magenta coloured points give the exact value of (29) for a raster of different φ . (The actual bound) The cyan coloured line gives a pessimistic lower bound (not assuming continuity) valid for a segment of length ε_0 centred around a specific φ . Fixing the width of a segment, ε_0 , to be fine enough will give a tighter lower bound. In order to perform the computation efficiently, we start with a rough raster with a large segment size. We then identify and refine the segment with the lowest estimate on the target function $H(Z|E\theta)$ and we repeat this procedure.

which means that we can perform optimisation (29) by replacing S with $S - 2\varepsilon_0$ on each segment of size $2\varepsilon_0$ (see Fig. 4) to obtain a reliable lower bound.

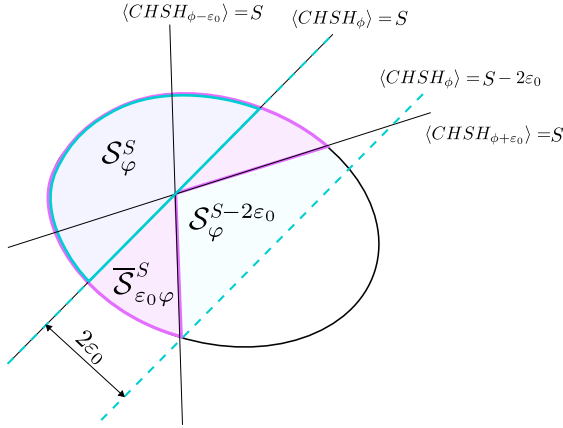


Fig. 4. **Feasible sets:** The optimisation for a fixed φ runs over a set \mathcal{S}_φ^S , i.e. all states with CHSH values larger than or equals to S . Varying φ by not more than ε_0 will not change the CHSH value by more than $2\varepsilon_0$. Therefore, the set $\mathcal{S}_\varphi^{S-2\varepsilon_0}$ includes all states that can attain CHSH value larger than or equals to S for some angle in the interval $(\varphi - \varepsilon_0, \varphi + \varepsilon_0)$.

We are now left with assessing the change in the objective of (29) introduced by varying φ , i.e. the error of the functional. Using Hölder's inequality, we can dualise the trace norm of an operator X as

$$\|X\|_1 = \sup_{Y: \|Y\|_\infty=1} \text{tr}(YX) \quad (46)$$

and for suitably chosen M, N with $\|M\|_\infty = \|N\|_\infty = 1$, we can rewrite the objective of (29) as

$$f_{M,N}(\varphi, \rho) := \langle \lambda \{M, Q(0)\} - \lambda Q(0)MQ(0) + (1 - \lambda) \{N, Q(\varphi)\} - (1 - \lambda)Q(\varphi)NQ(\varphi) \rangle_\rho \quad (47)$$

Here, we could bound the following expression by:

$$\begin{aligned}
& |f_{M,N}(\varphi, \rho) - f_{M,N}(\varphi + \varepsilon, \rho)| \\
& \leq (1 - \lambda) \sup_{N, \varphi, \varepsilon} \left\| \{N, Q(\varphi)\} - Q(\varphi)NQ(\varphi) - \{N, Q(\varphi + \varepsilon)\} + Q(\varphi + \varepsilon)NQ(\varphi + \varepsilon) \right\|_{\infty} \\
& \leq (1 - \lambda) 4\varepsilon_0
\end{aligned} \tag{48}$$

which follows after a short computation from the central estimate $\|(Q(\varphi) - Q(\varphi + \varepsilon))\|_{\infty} \leq \varepsilon_0/2$, which was already computed in (44).

Thus, by combining (44) and (48), we can estimate the maximal error on a segment around some fixed φ . Applying this estimate and the technique described above to (29), finally gives

$$\begin{aligned}
C_{\mathbb{C}^{4 \times 4}}^*(S) &= \inf_{\varphi \in [0, \pi/2]} \left[\inf_{\substack{(b_x, b_z) \\ b_x^2 + b_z^2 = 1}} \left[\inf_{\rho} \lambda \|\rho - T_0[\rho]\|_1 + (1 - \lambda) \|\rho - T_1[\rho]\|_1 \right. \right. \\
& \quad \left. \left. \text{s.th.: } \langle F_0 \rangle_{\rho} + b_x \langle F_x \rangle_{\rho} + b_z \langle F_z \rangle_{\rho} = S \right] \right] \\
&\geq \inf_{\varphi_k \in \mathcal{I}} \inf_l \left[\inf_{\rho} \lambda \|\rho - T_0[\rho]\|_1 + (1 - \lambda) \|\rho - T_1[\rho]\|_1 - 2(1 - \lambda) \varepsilon_0^k \right. \\
& \quad \left. \text{s.th.: } \langle F_0 \rangle_{\rho} + b_x \langle F_x \rangle_{\rho} + b_z \langle F_z \rangle_{\rho} = S - 2\varepsilon_0^k \right]
\end{aligned} \tag{49}$$

where ε_0^k denotes the according segment width and $\varphi_k \in \mathcal{I}$ denote the angles which form the raster as described above and in Fig. 3.

G. Worst case convex hull over two-qubit strategies:

By employing the techniques described in the previous subsections, we are able to compute the two-qubit function $C_{\mathbb{C}^{4 \times 4}}^*(S)$ point-wise up to arbitrary precision. The only remaining step for computing the desired bound $C^*(S)$ is to estimate (22). We will tackle this problem by defining a convex function $\overline{C}(S)$ that is smaller or equals to $C_{\mathbb{C}^{4 \times 4}}^*(S)$ for all $S \in (2, 2\sqrt{2})$, (see Fig. 5). Given such a function $\overline{C}(S)$, we can conclude that

$$\begin{aligned}
C^*(S) &= \inf_{\mu: \langle S' \rangle_{\mu} = S} \int_{S'=2}^{2\sqrt{2}} \mu(dS') C_{\mathbb{C}^{4 \times 4}}^*(S') \\
&\geq \inf_{\mu: \langle S' \rangle_{\mu} = S} \int_{S'=2}^{2\sqrt{2}} \mu(dS') \overline{C}(S') \\
&= \inf_{\mu: \langle S' \rangle_{\mu} = S} \overline{C} \left(\int_{S'=2}^{2\sqrt{2}} \mu(dS') S' \right) = \overline{C}(S).
\end{aligned} \tag{50}$$

At this point, we note that the analytical result of [4], which is a special case of our computation for $\lambda = 1$, shows that $C_{\mathbb{C}^{4 \times 4}}^*(S)$ is convex. This means that we can set $\overline{C}(S) = C_{\mathbb{C}^{4 \times 4}}^*(S)$ in the case of $\lambda = 1$. The numerical evaluation of $C_{\mathbb{C}^{4 \times 4}}^*(S)$ suggest the same conclusion might actually hold for all $\lambda \in (0, 1)$. However, we could not prove this analytically and therefore, the following steps is necessary.

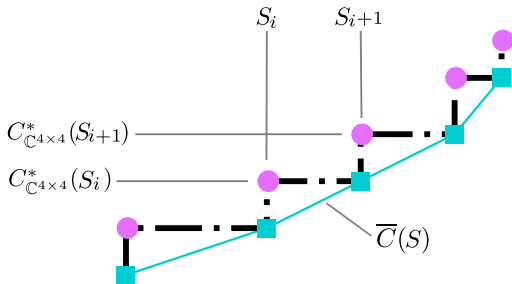


Fig. 5. **Convex bound:** given the value of $C_{\mathbb{C}^{4 \times 4}}^*(S)$ for a raster of values $\dots \leq S_i \leq S_{i+1} \leq \dots$ (magenta points) allows us to estimate $C_{\mathbb{C}^{4 \times 4}}^*(S)$ from below by taking the floor on every interval (dot-dashed black line). The extreme points of this graph are a subset of the points marked by cyan squares. From this we can easily compute the lower convex estimate $\overline{C}(S)$ (cyan line).

It is straight forward to see from the definition of (25) that $C_{\mathbb{C}^{4 \times 4}}^*(S)$ is a monotonous non-decreasing function, i.e. we have $C_{\mathbb{C}^{4 \times 4}}^*(S_1) \leq C_{\mathbb{C}^{4 \times 4}}^*(S_2)$ for $S_1 \leq S_2$, since increasing S will impose more restrictions on Eve leaving her with a

smaller set of possible attacks. The evaluation of $C_{\mathbb{C}^{4 \times 4}}^*(S)$ for a raster of values $S_0 = 2 \leq S_1 \leq S_2 \leq \dots \leq S_N = 2\sqrt{2}$ will therefore enable us to estimate $C_{\mathbb{C}^{4 \times 4}}^*(S)$ from below for all values of S by taking the floor

$$\lfloor C_{\mathbb{C}^{4 \times 4}}^*(S) \rfloor := C_{\mathbb{C}^{4 \times 4}}^*(S_i) \quad \forall S \in [S_i, S_{i+1}) \quad (51)$$

on every interval $[S_i, S_{i+1})$. Since this function is now defined on every S and is never larger than $C_{\mathbb{C}^{4 \times 4}}^*(S)$ itself, computing its lower convex hull by applying a Legendre transformation twice will give us a valid convex estimate $\overline{C}(S)$ (see Fig. 5).

H. A conjectured alternative proof

We observed from some numerical exploration that the states saturating optimisation (7) for $\lambda = 1/2$ appear to have the following two properties:

1. The reduced state on \mathcal{AB} is Bell-diagonal with only two nonzero eigenvalues.
2. The states satisfy $P_g(A_0|E) = P_g(A_1|E)$, where $P_g(A_X|E)$ is Eve's maximum probability of guessing the outcome of measurement A_X .

Letting $\rho_{E|A_X}$ denote Eve's state conditioned on the outcome A_X , the first property would imply $F(\rho_{E|A_X=0}, \rho_{E|A_X=1})^2 = 1 - d(\rho_{E|A_X=0}, \rho_{E|A_X=1})^2$, where F is the root-fidelity and d is the trace distance. (This is because Eve's states would then be supported on a common qubit subspace, and this equality holds for qubit states when the states have the same eigenvalues [14], which is indeed the case here [4].) Using the fact that we can assume A_X to be uniform without loss of generality, it would then follow from the bound in [15] and the relation $d(\rho_{E|A_X=0}, \rho_{E|A_X=1}) = 2P_g(A_X|E) - 1$ that

$$H(A_X|E) \geq \log(2) - h_2\left(\frac{1 - F(\rho_{E|A_X=0}, \rho_{E|A_X=1})}{2}\right) = \log(2) - h_2\left(\frac{1 - \sqrt{4P_g(A_X|E)(1 - P_g(A_X|E))}}{2}\right). \quad (52)$$

Applying the second property would then imply¹

$$\begin{aligned} \frac{1}{2}H(A_0|E) + \frac{1}{2}H(A_1|E) &\geq \log(2) - h_2\left(\frac{1 - \sqrt{4P_g(A_X|E)(1 - P_g(A_X|E))}}{2}\right) \text{ for either } X \\ &= \log(2) - h_2\left(\frac{1 - \sqrt{4P_g^{\text{avg}}(1 - P_g^{\text{avg}})}}{2}\right), \text{ where } P_g^{\text{avg}} = \frac{1}{2}P_g(A_0|E) + \frac{1}{2}P_g(A_1|E). \end{aligned} \quad (53)$$

The key point of this reduction is that the maximum value of P_g^{avg} (subject to a constraint on the CHSH value) can be bounded by SDP methods [16–18]. We computed the corresponding bounds, and found that they matched closely with the results obtained above. Hence if it could be proven that the two properties listed above indeed hold for the states saturating the optimisation in (7), this would provide an alternative approach to deriving our results. The benefit of such an approach is that it would be substantially faster, as it does not rely on computing an ε -net of points.

We remark that for the case $\lambda = 1$ (i.e. simply bounding the $H(A_0|E)$ term alone), we can prove that the first property holds, and thus Eq. (52) must hold in that scenario. In that case, we find that substituting the known closed-form bound on $P_g(A_0|E)$ in terms of the CHSH value [19] yields exactly the closed-form bound on $H(A_0|E)$ derived in Ref. [4]. This can be viewed as an alternative method to derive the latter bound, and it may be of interest to study how this approach could be generalised.

I. Approaches without the qubit reduction

Our analysis thus far relied on reducing the analysis to a qubit scenario. In principle, however, there are some approaches which could be used to tackle the optimisation (7) without this reduction, and we shall now briefly outline these possibilities. These approaches could potentially allow for more general applicability of our methods.

¹ If the bound (52) were convex with respect to $P_g(A_X|E)$, the second property would not be required; unfortunately, the bound is instead concave, so instead this approach only yields the desired final result *if and only if* the second property holds.

The first approach consists of noting that the trace norm terms in the optimisation (29) can be rewritten using

$$\|\rho - T[\rho]\|_1 = \sup_{-1 \leq M \leq 1} \text{tr}(M(\rho - T[\rho])) = \sup_P \frac{1}{\|P\|_\infty} \text{tr}(P(\rho - T[\rho])) = \sup_P \frac{1}{\|P\|_\infty} \text{tr}((P - T[P])\rho), \quad (54)$$

where \sup_P is taken over all Hermitian P , and for the last equality we used the fact that pinching channels are self-adjoint. Therefore, any choice of P yields a valid lower bound. In particular, if we choose P to be a (noncommutative) polynomial function of the measurement operators, then lower-bounding $\text{tr}((P - T[P])\rho)$ is precisely a noncommutative polynomial optimisation of the type studied in [18], which can be solved by SDP methods *without* reducing the analysis to qubits. An advantage of this approach is that we can impose the full output statistics as constraints (similar to [1, 16, 17]) instead of just the CHSH value alone. As for the $\|P\|_\infty$ term, it can be upper-bounded separately by noting that $\|P\|_\infty = \sup_\sigma |\text{tr}(P\sigma)| \leq \max\{\sup_\sigma \text{tr}(P\sigma), \sup_\sigma \text{tr}(-P\sigma)\}$, where \sup_σ is taken over all normalised density operators σ . This is also of the right form to be bounded using the SDP method described in [18]. If P is chosen to be a polynomial of low degree, the corresponding SDPs are quite tractable and can be solved quickly (in particular, they are substantially simpler than the ones described in [1]).

Unfortunately, when we applied this method to the CHSH scenario, we were unable to find a choice of P that was sufficiently robust to noise for practical purposes. While we did find that it can yield a tight bound at maximum CHSH value, the bound quickly drops to zero once noise is added. It is not currently clear whether this is an inherent limitation of this approach, or whether some better choice of P might overcome this difficulty. (A possible cause of this suboptimality could be the fact that since the optimisations for $\text{tr}((P - T[P])\rho)$ and $\|P\|_\infty$ were solved separately, this “decouples” them from each other, resulting in worse bounds than would be obtained from tackling (54) directly. The choice of P that certifies a tight bound at maximum CHSH violation was obtained by exploiting the fact that the states and measurements which attain maximum CHSH value are essentially unique, up to trivial local operations. Therefore, we were able to find an explicit operator P that saturates the variational characterisation in Eq. (54) and write it as a polynomial of those measurement operators. However, some care was still needed to choose the polynomial such that the bound on $\|P\|_\infty$ is tight.)

A second approach is based on the method developed in [1]. To briefly summarise, the method described in that work essentially yields some possible choices of vector $\vec{\mu}$ and operator polynomials K_0, K_1 such that

$$H(A_X|E) \geq \vec{\mu} \cdot \vec{\gamma} - \log\langle K_X \rangle, \quad (55)$$

where $\vec{\gamma}$ is the list of all statistics estimated in the experiment (which could be, for instance, just the CHSH value alone but could also be all output statistics instead). We now note that for any $\alpha > 0$, we have $\log x \leq x/\alpha + \log \alpha - 1$ (this is simply the tangent line to $\log x$ at the point $x = \alpha$). Therefore, for any α_0, α_1 we would have

$$\lambda H(A_0|E) + (1 - \lambda)H(A_1|E) \geq \lambda(\vec{\mu} \cdot \vec{\gamma} - \log\langle K_0 \rangle) + (1 - \lambda)(\vec{\mu} \cdot \vec{\gamma} - \log\langle K_1 \rangle) \quad (56)$$

$$\geq \vec{\mu} \cdot \vec{\gamma} - \left\langle \frac{\lambda}{\alpha_0} K_0 + \frac{1 - \lambda}{\alpha_1} K_1 \right\rangle - \lambda \log \alpha_0 - (1 - \lambda) \log \alpha_1 + 1. \quad (57)$$

In this final expression, $\langle (\lambda/\alpha_0)K_0 + ((1 - \lambda)/\alpha_1)K_1 \rangle$ is again an operator polynomial of a form which can be bounded using the SDPs in [18] without requiring the qubit reduction. By optimising over choices of the two tangent points α_X (as well as the vector $\vec{\mu}$ and operator polynomials K_X), we were able to compute some bounds on the main optimisation (7), imposing constraints based on the full output statistics. However, we found that while the resulting bounds are indeed better than the bounds on $H(A_0|E)$ alone, the improvement was fairly small (in particular, the resulting curves were worse than those shown in the main text). Hence we were also unable to use this approach to obtain tight bounds in this situation, though in contrast to the first approach above, it performs well at moderate noise values rather than low noise values. Again, it is not currently clear whether it might be possible to improve on this finding with a better choice of the variational parameters $\alpha_X, \vec{\mu}, K_X$. (In fact, the parameter $\vec{\mu}$ could also be optimised separately for each term $H(A_X|E)$, but this is computationally expensive.)

II. SIMULATION WITH ALL-PHOTONIC SETUP

In this section, we present the simulated asymptotic key rate that one could achieve in an all-photon experiment. For all-photon implementations the noise model presented in Ref. [20] gives a more realistic description than the white noise considered in the main text. In this model, the source is modelled by a pair of two-mode squeeze vacua (TMSV) over polarisation modes with mean photon number λ_1 and λ_2 . Alice and Bob will then set the measurement angles to be θ_{A_X} and θ_{B_Y} where $X \in \{0, 1\}$ and $Y \in \{0, 1, 2, 3\}$ are their corresponding inputs. Both Alice and Bob will have a pair of single-photon detectors, each with some imperfect quantum efficiency. We let the effective detection efficiency (the total transmittivity between the source and each detector) be η . Furthermore, we assume that Alice and Bob will

give deterministic outputs whenever they observe no detection events. Finally, we also assume that the detectors have negligible dark count rates.

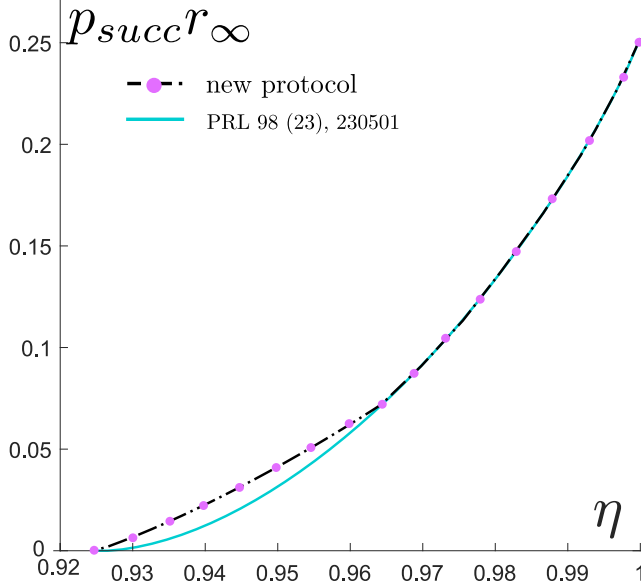


Fig. 6. **Asymptotic key rate for all-photonic experiments.** For this simulation, we use the model presented in Ref. [20] and set the dark count rate of the detectors to zero. We also assumed that Alice and Bob assign deterministic outputs whenever their detectors do not click. We plot the lower bound on the key rate as a function of detection efficiency η . From the plot, we can see that randomised key basis can improve the achievable key rate in the lower detection efficiency regime.

The corresponding key rate is presented in Fig. 6. To obtain these curves, we optimise the achievable key rates by varying the mean photon number of the TMSV λ_1 and λ_2 as well as the measurement angles of Alice and Bob θ_{Ax} θ_{By} for each value of η . Unfortunately, the improvement from employing the randomised key basis protocol is rather limited for the all-photonic experiments. Remarkably, the required detection efficiency to achieve non-zero key rate remains extremely demanding.

III. ADDITIONAL LEMMAS AND THEOREMS

Theorem 1 DI-Binary Pinsker++: (The following Thm. is a special case of Thm.1 in [10]) Let Q be a (not necessarily rank one) projector on a finite dimensional Hilbert space of dimension d and let T be the pinching channel constructed from Q via

$$T[\rho] = Q\rho Q + (\mathbf{1} - Q)\rho(\mathbf{1} - Q) = \rho + 2Q\rho Q - \{Q, \rho\}. \quad (58)$$

For any state ρ , the following inequality holds:

$$D(\rho \| T[\rho]) \geq \log(2) - h_2\left(\frac{1 - \|\rho - T[\rho]\|_1}{2}\right). \quad (59)$$

For the proof of Thm. 1, we will require the following Lemmas:

Lemma 1 Gibbs variational principle for operators: Let L be a self-adjoint operator. For any quantum state ρ , the following holds:

$$-\text{tr}(\rho L) \geq H(\rho) - \log \text{tr}(e^L). \quad (60)$$

Proof. Consider the thermal state $\sigma = \frac{e^L}{\text{tr}(e^L)}$.

$$-\text{tr}(\rho L) = -\text{tr}(\rho \log e^L) \quad (61)$$

$$= -\text{tr}\left(\rho \left(\log \frac{e^L}{\text{tr}(e^L)} + \log \text{tr}(e^L)\right)\right) \quad (62)$$

$$= -\text{tr}\left(\rho \log \frac{e^L}{\text{tr}(e^L)}\right) - \text{tr}(\rho \log \text{tr}(e^L)) \quad (63)$$

$$= -\text{tr}(\rho \log \sigma) - \log \text{tr}(e^L) \quad (64)$$

$$\geq -\text{tr}(\rho \log \rho) - \log \text{tr}(e^L) \quad (65)$$

$$= H(\rho) - \log \text{tr}(e^L), \quad (66)$$

where we have used the positivity of the quantum relative entropy $D(\rho||\sigma) = \text{tr}(\rho \log \rho - \rho \log \sigma)$. \square

Lemma 2 : For a quantum state χ and an operator A with spectral radius $r_{\text{spec}}(A) \leq s$, the following relation holds:

$$\text{tr}(\chi e^A) \leq \cosh(s) + \frac{1}{s} \sinh(s) \text{tr}(\chi A). \quad (67)$$

Proof. Firstly, we will find an upper bound to the exponential function in a fixed interval $[-s, s]$. The simplest ansatz is to upper bound it with a linear function, which can be parameterised with α and β such that $e^x \leq \alpha + \beta x$. Such an upper bound can be determined by demanding that the points of the exponential function at the boundaries of the interval intersects with the linear function, i.e.

$$\alpha \pm \beta s = e^{\pm s}, \quad (68)$$

which yields $\alpha = \cosh(s)$, $\beta = \frac{1}{s} \sinh(s)$. Hence, we obtain

$$\text{tr}(\chi e^A) \leq \text{tr}\left(\chi \left[\cosh(s) + \frac{1}{s} \sinh(s) A\right]\right) \quad (69)$$

$$= \cosh(s) + \frac{1}{s} \sinh(s) \text{tr}(\chi A). \quad (70)$$

\square

Lemma 3 : For any projector Q and quantum state ρ , we have

$$\|\rho - T[\rho]\|_1 \leq 1 \quad (71)$$

Proof. We use equation (46) and projectors P and $M = 2P - \mathbf{1}$ to rewrite

$$\begin{aligned} \sup_{\rho, Q} \|\rho - T[\rho]\|_1 &= 2 \sup_{\rho, P, Q} \text{tr}(P(\rho - T[\rho])) \\ &= 2 \sup_{\rho, P, Q} \langle \{P, Q\} - 2QPQ \rangle_\rho \\ &= 2 \sup_{P, Q} \|\{P, Q\} - 2QPQ\|_\infty \end{aligned} \quad (72)$$

Using the usual block decomposition of the algebra generated by two projectors (P and Q) we can conclude that the optimal solution of the above will be attained on 2×2 matrices. We can assume without loss of generality that

$$P = \begin{pmatrix} 1 & 0 \\ 0 & 0 \end{pmatrix} \text{ and } Q = \begin{pmatrix} \cos(\phi)^2 & \cos(\phi) \sin(\phi) \\ \cos(\phi) \sin(\phi) & \sin(\phi)^2 \end{pmatrix}. \quad (73)$$

Thus, we have

$$\begin{aligned} &\sup_{\phi} \left\| \left\{ \begin{pmatrix} 1 & 0 \\ 0 & 0 \end{pmatrix}, \begin{pmatrix} \cos(\phi)^2 & \cos(\phi) \sin(\phi) \\ \cos(\phi) \sin(\phi) & \sin(\phi)^2 \end{pmatrix} \right\} \right. \\ &\quad \left. - 2 \begin{pmatrix} \cos(\phi)^2 & \cos(\phi) \sin(\phi) \\ \cos(\phi) \sin(\phi) & \sin(\phi)^2 \end{pmatrix} \begin{pmatrix} 1 & 0 \\ 0 & 0 \end{pmatrix} \begin{pmatrix} \cos(\phi)^2 & \cos(\phi) \sin(\phi) \\ \cos(\phi) \sin(\phi) & \sin(\phi)^2 \end{pmatrix} \right\|_\infty \\ &= \frac{1}{2}. \end{aligned} \quad (74)$$

\square

Proof of Pinsker++. The basic idea of this proof is to find a lower bound on $D(\rho||T[\rho])$ in terms of $\|\rho - T[\rho]\|_1$ by bounding the expression

$$\inf_{\rho} D(\rho||T[\rho]) - \lambda \|\rho - T[\rho]\|_1 \geq c_\lambda \quad (75)$$

from below by some c_λ that only depends on a variational parameter $\lambda \in \mathbb{R}^+$ but not on ρ . Given such a c_λ for all λ will then allow us to obtain a bound on D via an inverse Legendre transformation

$$\forall \rho : \quad D(\rho||T[\rho]) \geq \sup_{\lambda \in \mathbb{R}^+} c_\lambda + \lambda \|\rho - T[\rho]\|_1 := f(\|\rho - T[\rho]\|_1) \quad (76)$$

Rewriting (75) with equation (46), $M = 2P - \mathbf{1}$ and Lem. 1 for $L = \log(T[\rho]) + 2\lambda(P - T[P])$ yields the following inequality:

$$\begin{aligned}
& D(\rho \| T[\rho]) - \lambda \|\rho - T[\rho]\|_1 \\
& \geq \inf_{\rho} \inf_{0 \leq P \leq \mathbb{I}} -\text{tr}(\rho(\log(T[\rho]) + 2\lambda(P - T[P]))) - H(\rho) \\
& \geq \inf_{\rho} \inf_{0 \leq P \leq \mathbb{I}} -\log \text{tr} \left(e^{\log(T[\rho]) + 2\lambda(P - T[P])} \right) \\
& \geq -\log \sup_{\rho} \sup_{0 \leq P \leq \mathbb{I}} \text{tr} \left(e^{\log(T[\rho]) + 2\lambda(P - T[P])} \right) \\
& \geq -\log \sup_{\rho} \sup_{0 \leq P \leq \mathbb{I}} \text{tr} \left(e^{\log(T[\rho])} e^{2\lambda(P - T[P])} \right) \\
& = -\log \sup_{\rho} \sup_{0 \leq P \leq \mathbb{I}} \text{tr} \left(T[\rho] e^{2\lambda(P - T[P])} \right), \tag{77}
\end{aligned}$$

where we have applied the Golden-Thompson inequality $\text{tr}(e^{A+B}) \leq \text{tr}(e^A e^B)$. Next, we use Lem. 2 with $\chi = T[\rho]$, $A = 2\lambda(P - T[P])$, which implies $s = \lambda$ (see Lem. 3). This yields

$$\begin{aligned}
\text{Eq. (77)} & \geq -\log \left(\cosh(s) + \sup_{\rho} \sup_{0 \leq P \leq \mathbb{I}} \frac{2\lambda}{s} \sinh(s) \text{tr}(T[\rho](P - T[P])) \right) \\
& = -\log(\cosh(\lambda)) \tag{78}
\end{aligned}$$

Hence, we know that

$$D(\rho \| T[\rho]) \geq -\log(\cosh(\lambda)) + \lambda \|\rho - T[\rho]\|_1. \tag{79}$$

Since this is true for all $\lambda \geq 0$, the optimal bound can be found by maximizing the right hand side over $\lambda \geq 0$, which gives

$$\lambda_{\max} = \text{arccoth} \left(\frac{1}{\|\rho - T[\rho]\|_1} \right). \tag{80}$$

Inserting it back into (79), where we use the notation $x = \|\rho - T[\rho]\|_1$, yields

$$D(\rho \| T[\rho]) \geq -\log \left(\cosh \left(\text{arccoth} \left(\frac{1}{x} \right) \right) \right) + x \text{arccoth} \left(\frac{1}{x} \right) \tag{81}$$

$$= \frac{1}{2} \left(\log(1 - x^2) + x \log \left(\frac{1+x}{1-x} \right) \right) \tag{82}$$

$$= \frac{1}{2} (\log(1+x) + \log(1-x) + x \log(1+x) - x \log(1-x)) \tag{83}$$

$$= \frac{1+x}{2} \log(1+x) + \frac{1-x}{2} \log(1-x) \tag{84}$$

$$= \log(2) + \frac{1+x}{2} \log \left(\frac{1+x}{2} \right) + \frac{1-x}{2} \log \left(\frac{1-x}{2} \right) \tag{85}$$

$$= \log(2) - h_2 \left(\frac{1-x}{2} \right), \tag{86}$$

which concludes the proof. \square

-
- [1] Tan, E. Y.-Z., Schwonnek, R., Goh, K. T., Primateamaja, I. W. & Lim, C. C.-W. Computing secure key rates for quantum key distribution with untrusted devices. *arXiv preprint arXiv:1908.11372v1* (2019).
 - [2] Coles, P. J. Unification of different views of decoherence and discord. *Physical Review A* **85**, 042103 (2012).
 - [3] Coles, P. J., Metodiev, E. M. & Lütkenhaus, N. Numerical approach for unstructured quantum key distribution. *Nature Communications* **7**, 11712 (2016).

- [4] Pironio, S. *et al.* Device-independent quantum key distribution secure against collective attacks. *New Journal of Physics* **11**, 045021 (2009).
- [5] Araki, H. & Lieb, E. H. Entropy inequalities. *Communications in Mathematical Physics* **18**, 160–170 (1970).
- [6] Jordan, C. Essai sur la géométrie à n dimensions. *Bulletin de la Société mathématique de France* **3**, 103–174 (1875).
- [7] Halmos, P. R. Two subspaces. *Transactions of the American Mathematical Society* **144**, 381–389 (1969).
- [8] Masanes, L. Asymptotic violation of bell inequalities and distillability. *Physical Review Letters* **97**, 050503 (2006).
- [9] Bottcher, A. & Spitkovsky, I. A gentle guide to the basics of two projections theory. *Linear Algebra and its Applications* **432**, 1412 – 1459 (2010).
- [10] Schwonnek, R. & Wolf, R. Pinsker’s inequality for a quantum channel. In preparation.
- [11] Boyd, S. & Vandenberghe, L. *Convex Optimization* (Cambridge University Press, 2004).
- [12] Schwonnek, R., Dammeier, L. & Werner, R. F. State-independent uncertainty relations and entanglement detection in noisy systems. *Physical Review Letters* **119**, 170404 (2017).
- [13] Zhao, Y.-Y. *et al.* Entanglement detection by violations of noisy uncertainty relations: A proof of principle. *Physical Review Letters* **122**, 220401 (2019).
- [14] Tan, E. Y.-Z., Lim, C. C.-W. & Renner, R. Advantage Distillation for Device-Independent Quantum Key Distribution. *Physical Review Letters* **124**, 020502 (2020).
- [15] Roga, W., Fannes, M. & Życzkowski, K. Universal Bounds for the Holevo Quantity, Coherent Information, and the Jensen-Shannon Divergence. *Physical Review Letters* **105**, 040505 (2010).
- [16] Bancal, J.-D., Sheridan, L. & Scarani, V. More randomness from the same data. *New Journal of Physics* **16**, 033011 (2014).
- [17] Nieto-Silleras, O., Pironio, S. & Silman, J. Using complete measurement statistics for optimal device-independent randomness evaluation. *New Journal of Physics* **16**, 013035 (2014).
- [18] Navascués, M., Pironio, S. & Acín, A. A convergent hierarchy of semidefinite programs characterizing the set of quantum correlations. *New Journal of Physics* **10**, 073013 (2008).
- [19] Masanes, L., Pironio, S. & Acín, A. Secure device-independent quantum key distribution with causally independent measurement devices. *Nature Communications* **2**, 238 (2011).
- [20] Tsujimoto, Y. *et al.* Optimal conditions for the Bell test using spontaneous parametric down-conversion sources. *Physical Review A* **98**, 063842 (2018).

